Electronic Supplementary Information

Stereoselective synthesis of oxime containing Pd(II) compounds: Highly effective, selective and stereo-regulated cytotoxicity against carcinogenic PC-3 cells

Isabel de la Cueva-Alique,[a] Elena de la Torre-Rubio,[a] Laura Muñoz-Moreno,[b] Alicia Calvo-Jareño,[a] Adrián Pérez-Redondo,[a] Lourdes Gude,[a] Tomás Cuenca,[a] Eva Royo*[a]

[a] Universidad de Alcalá, Instituto de Investigación Química "Andrés M. del Río" (IQAR), Departamento de Química Orgánica y Química Inorgánica, 28805 Alcalá de Henares, Madrid, Spain

[b] Departamento de Biología de Sistemas, Facultad de Medicina y Ciencias de la Salud, Universidad de Alcalá, 28805 Alcalá de Henares, Madrid, Spain

Selected characterization data:

Selected FRET DNA melting assay data:

Figure S54: FRET DNA melting curves of **2a**, **2a'**, **2b and 2b'** with representative ds DNA (F10T)

Cell cycle assay data:

Figure S55: Analysis of cell cycle of PC-3 cells after treatment with cisplatin, **2a** and **2a'**.

Table S1. Selected Lengths (Å) and Angles (deg) for **1a-1** and **1a'-1**.

	1a-1	**1a'-1**
Pd(1)–Cl(1)	2.274(2)	2.273(2)
Pd(1)–Cl(2)	2.294(2)	2.294(2)
Pd(1)–N(1)	2.048(5)	2.046(5)
Pd(1)–N(2)	1.992(6)	1.990(6)
N(2)–O(1)	1.378(7)	1.379(7)
C(1)–C(2)	1.532(9)	1.519(9)
Cl(1)–Pd(1)–Cl(2)	92.9(1)	92.9(1)
Cl(1)–Pd(1)–N(1)	92.0(2)	92.0(2)
Cl(1)–Pd(1)–N(2)	172.3(2)	172.3(2)
Cl(2)–Pd(1)–N(1)	173.5(2)	173.7(2)
Cl(2)–Pd(1)–N(2)	94.0(2)	94.0(2)
N(1)–Pd(1)–N(2)	81.3(2)	81.4(2)
Pd(1)–N(1)–C(1)	108.8(4)	108.7(4)
Pd(1)–N(2)–C(2)	118.7(5)	118.4(5)
N(1)–C(1)–C(2)	108.0(5)	108.3(5)
N(2)–C(2)–C(1)	116.1(6)	116.4(6)

Table S2. Selected Lengths (Å) and Angles (deg) for **1b**.

1b-1		**1b-2**	
Pd(1)–Cl(1)	2.297(2)	Pd(2)–Cl(11)	2.278(3)
Pd(1)–Cl(2)	2.293(2)	Pd(2)–Cl(12)	2.297(2)
Pd(1)–N(1)	2.049(7)	Pd(2)–N(11)	2.052(8)
Pd(1)–N(2)	1.996(7)	Pd(2)–N(12)	1.972(7)
N(2)–O(1)	1.371(8)	N(12)–O(11)	1.381(9)
C(1)–C(2)	1.506(12)	C(21)–C(22)	1.524(12)
Cl(1)–Pd(1)–Cl(2)	94.8(1)	Cl(11)–Pd(2)–Cl(12)	91.8(1)
Cl(1)–Pd(1)–N(1)	92.7(2)	Cl(11)–Pd(2)–N(11)	98.4(2)
Cl(1)–Pd(1)–N(2)	173.1(2)	Cl(11)–Pd(2)–N(12)	177.5(2)
Cl(2)–Pd(1)–N(1)	172.1(2)	Cl(12)–Pd(2)–N(11)	169.6(2)
Cl(2)–Pd(1)–N(2)	91.9(2)	Cl(12)–Pd(2)–N(12)	90.7(2)
N(1)–Pd(1)–N(2)	80.7(3)	N(11)–Pd(2)–N(12)	79.1(3)
Pd(1)–N(1)–C(1)	107.1(5)	Pd(2)–N(11)–C(21)	108.6(5)
Pd(1)–N(2)–C(2)	118.7(6)	Pd(2)–N(12)–C(22)	120.0(6)
N(1)–C(1)–C(2)	109.8(7)	N(11)–C(21)–C(22)	106.4(7)
N(2)–C(2)–C(1)	114.8(8)	N(12)–C(22)–C(21)	114.6(8)

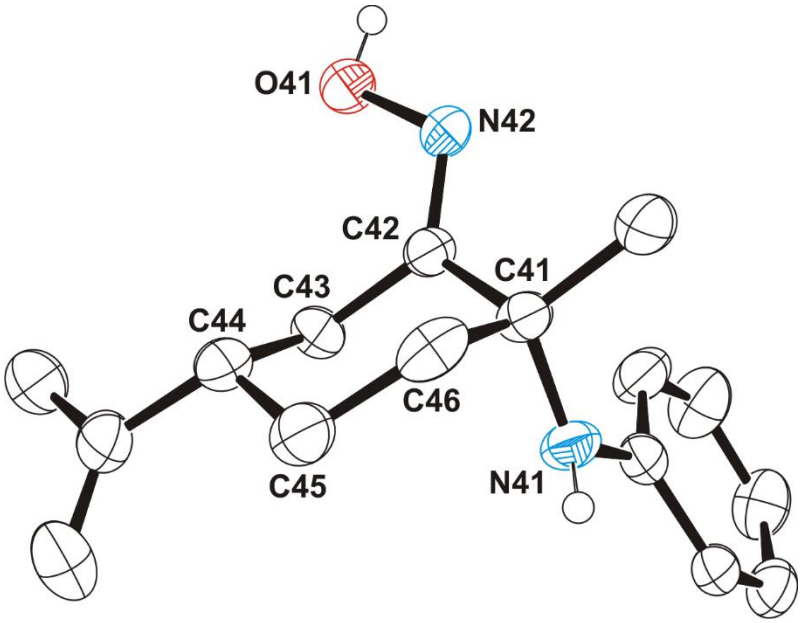

Figure S1. ORTEP drawing of the ligand which crystallized with compound **2a'** with 50% probability ellipsoids. Hydrogens bonded to carbon atoms have been omitted for clarity.

Table S3. Selected Lengths (Å) and Angles (deg) for **2a'**.

Pd(1)–N(1)	2.077(3)	Pd(1)–N(21)	2.080(3)
Pd(1)–N(2)	1.973(3)	Pd(1)–N(22)	1.976(3)
N(2)–O(1)	1.355(4)	N(22)–O(21)	1.343(4)
C(1)–C(2)	1.507(6)	C(21)–C(22)	1.511(6)
N(42)–O(41)	1.416(5)	C(41)–C(42)	1.517(6)
N(1)–Pd(1)–N(2)	81.4(1)	N(21)–Pd(1)–N(22)	81.1(1)
N(1)–Pd(1)–N(21)	101.2(1)	N(2)–Pd(1)–N(22)	95.9(1)
N(1)–Pd(1)–N(22)	176.2(1)	N(2)–Pd(1)–N(21)	172.6(1)
Pd(1)–N(1)–C(1)	110.7(2)	Pd(1)–N(21)–C(21)	107.7(2)
Pd(1)–N(2)–C(2)	118.6(3)	Pd(1)–N(22)–C(22)	119.0(3)
N(1)–C(1)–C(2)	109.3(3)	N(21)–C(21)–C(22)	108.7(3)
N(2)–C(2)–C(1)	117.1(4)	N(22)–C(22)–C(21)	116.3(4)
N(41)–C(41)–C(42)	111.7(4)	N(42)–C(42)–C(41)	117.3(4)

Table S4. Relevant hydrogen bonds[a] for compounds **1a-1**, **1a'-1**, **1b-1**, **1b-2** and **2a'**

Compound	D–H···A	D···A/Å	H···A/Å	D–H···A/deg
1a-1	O(1)–H(1)···Cl(2)	3.182(6)		
1a'-1	O(1)–H(1)···Cl(2)	3.179(6)		
1b-1	O(1)–H(1)···Cl(2)	3.086(7)		
1b-2	O(11)–H(11)···Cl(12)	2.999(7)		
2a'	O(1)–H(1)···O(21)	2.438(4)	1.36(6)	173(5)

[a]A = acceptor; D = donor.

Single-crystal X-ray diffraction data:

Table S5. Experimental data for the X-ray diffraction studies on **1a-1, 1a'-1, 1b** and **2a'**.

	1a-1·2CHCl$_3$	**1a'-1**·2CHCl$_3$	**1b**	**2a'**·C$_{16}$H$_{22}$N$_2$O
CCDC code	2129232	2129233	2129234	2129235
Formula	$C_{18}H_{24}Cl_8N_2OPd$	$C_{18}H_{24}Cl_8N_2OPd$	$C_{17}H_{24}Cl_2N_2OPd$	$C_{48}H_{65}ClN_6O_3Pd$
M_r	674.39	674.39	449.68	915.91
T [K]	200(2)	200(2)	200(2)	200(2)
λ[Å]	0.71073	0.71073	0.71073	0.71073
crystal system	Monoclinic	Monoclinic	Orthorhombic	Orthorhombic
space group	$P2_1$	$P2_1$	$P2_12_12_1$	$P2_12_12_1$
a [Å]; α [º]	8.409(1)	8.407(1)	10.597(1)	13.050(1)
b [Å]; β [º]	12.953(2); 96.87(1)	12.955(1); 96.86(1)	12.258(1)	15.813(1)
c [Å]; γ [º]	12.427(1)	12.424(1)	28.259(2)	22.414(1)
V [Å^3]	1343.8(2)	1343.5(2)	3670.5(6)	4625.1(7)
Z	2	2	8	4
ρ_{calcd} [g cm^{-3}]	1.667	1.667	1.627	1.315
$\mu_{MoK\alpha}$ [mm^{-1}]	1.500	1.500	1.307	0.506
F(000)	672	672	1824	1928
crystal size [mm^3]	0.40×0.21×0.17	0.34×0.23×0.19	0.26×0.24×0.16	0.24×0.18×0.16
θ range (deg)	3.11 to 27.50	3.11 to 27.50	3.32 to 27.50	3.01 to 27.50
index ranges	-10 to 10, -16 to 16, -16 to 16	-10 to 10, -16 to 16, -16 to 16	-13 to 13, -15 to 15, -36 to 33	-16 to 16, -20 to 20, -28 to 29
Reflections collected	29581	30348	45975	58204
Unique data	6100 [R_{int} = 0.074]	6157 [R_{int} = 0.058]	8411 [R_{int} = 0.086]	10580 [R_{int} = 0.055]
obsd data [I>2σ(I)]	5146	5139	6361	8989
Goodness-of-fit on F^2	1.166	1.132	1.087	1.101
final R[a] indices [I>2σ(I)]	R1 = 0.042, wR2 = 0.086	R1 = 0.040, wR2 = 0.078	R1 = 0.053, wR2 = 0.095	R1 = 0.037, wR2 = 0.064
R[a] indices (all data)	R1 = 0.062, wR2 = 0.098	R1 = 0.062, wR2 = 0.090	R1 = 0.087, wR2 = 0.109	R1 = 0.055, wR2 = 0.071
largest diff. peak/hole[e.Å^{-3}]	1.892/-1.157	1.796/-0.757	1.019/-0.842	0.700/-0.494

[a] $R1=\Sigma||F_0|-|F_c||/[\Sigma|F_0|]$ $wR2=\{[\Sigma w(F_0^2-F_c^2)^2]/[\Sigma w(F_0^2)^2]\}^{1/2}$

Figure S2. Numbering of cyclohexane skeleton of amino oxime proligands.

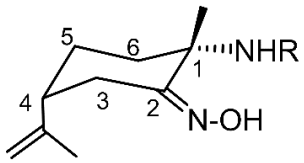

R = Ph (**a**), Bn (**b**)

Figure S3.^{1}H NMR spectrum of **a** in $CDCl_3$.[1]

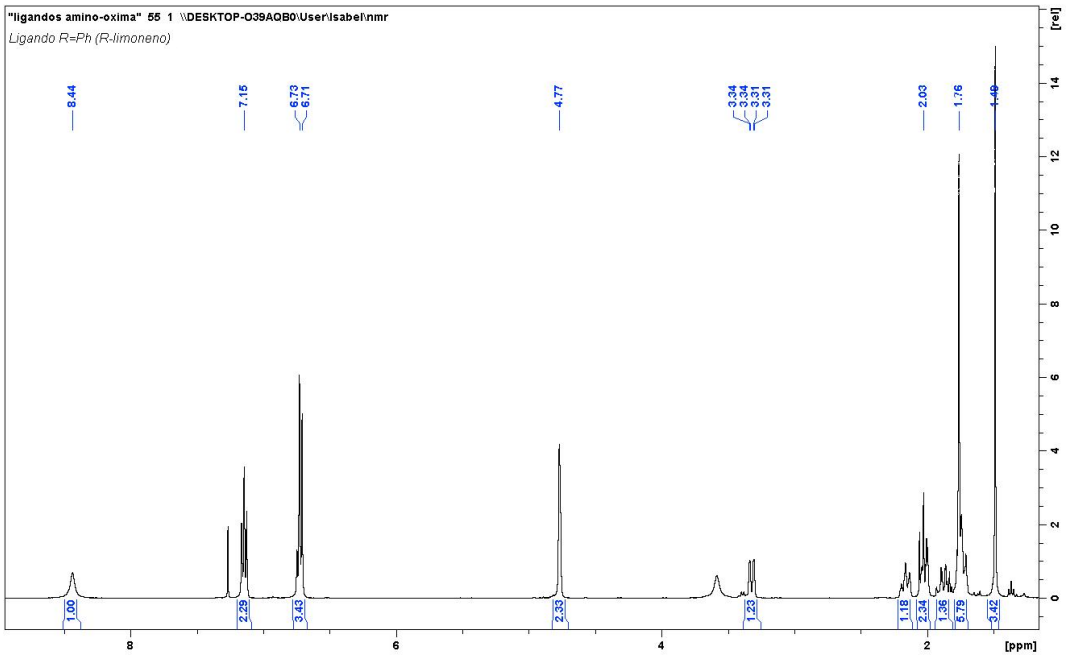

Figure S4.^{1}H NMR spectrum of **a'** in $CDCl_3$.

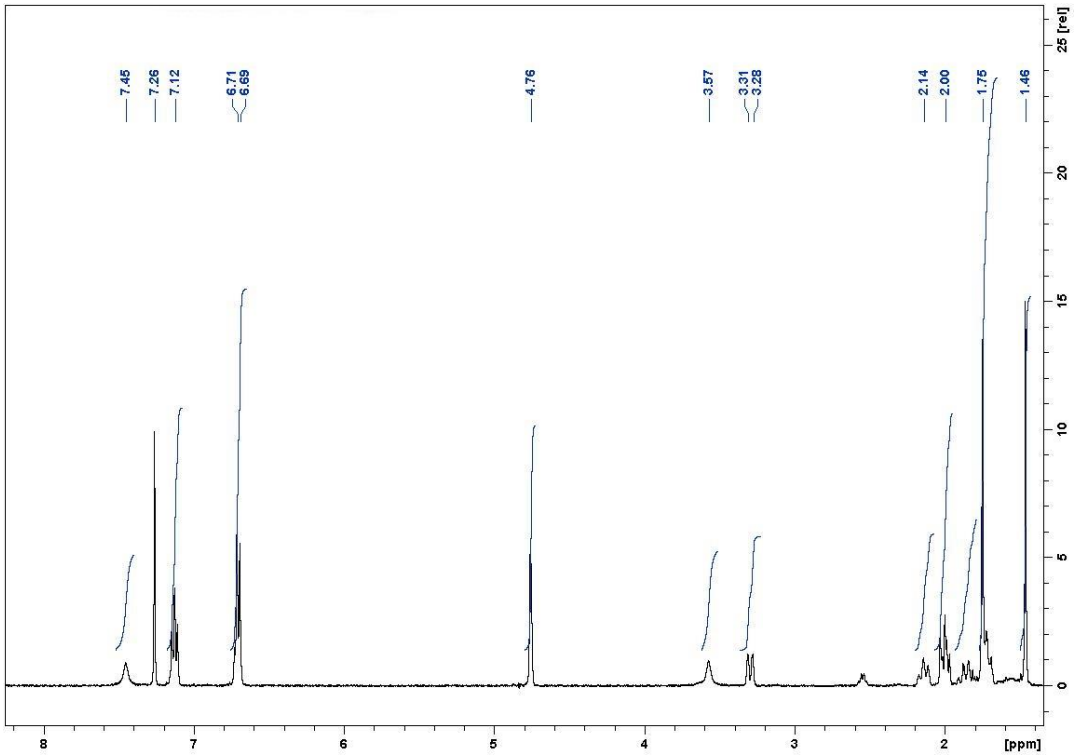

[1] Chemical shifts of NO<u>H</u> and N<u>H</u> protons can vary depending on the sample concentration. This behavior is also observed in NMR spectra of oxime metal compounds.

Figure S5. ^{1}H NMR spectrum of **b** in $CDCl_3$.

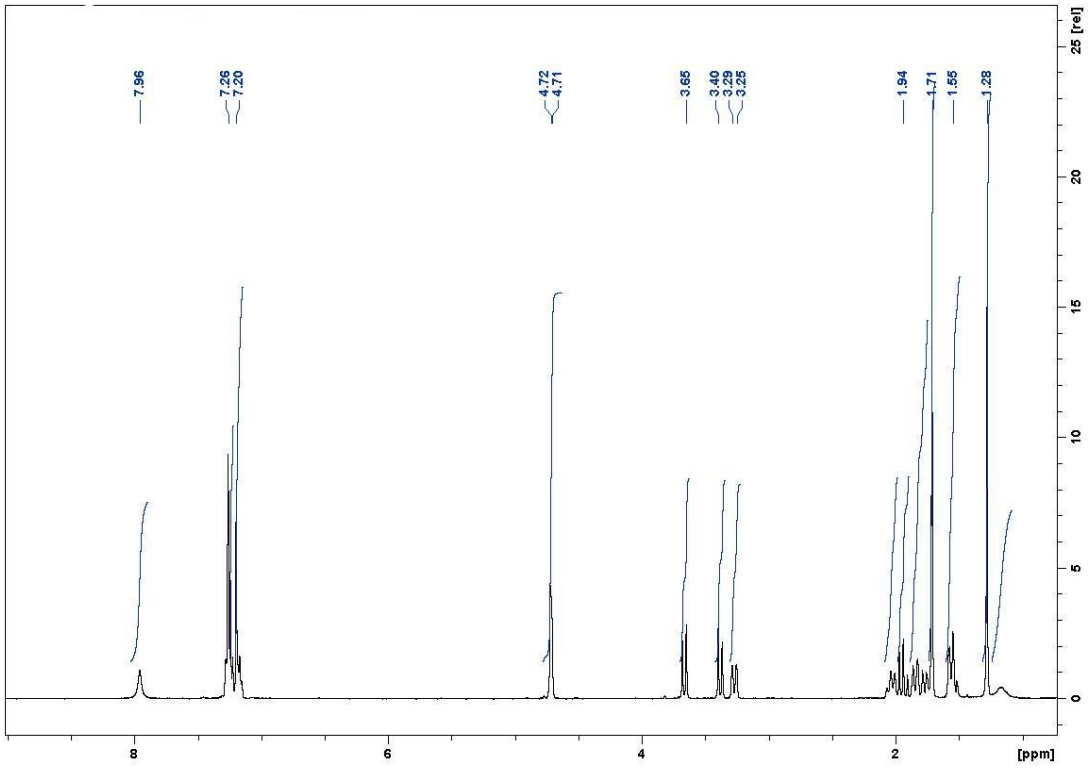

Figure S6. ^{1}H NMR spectrum of **b'** in $CDCl_3$.

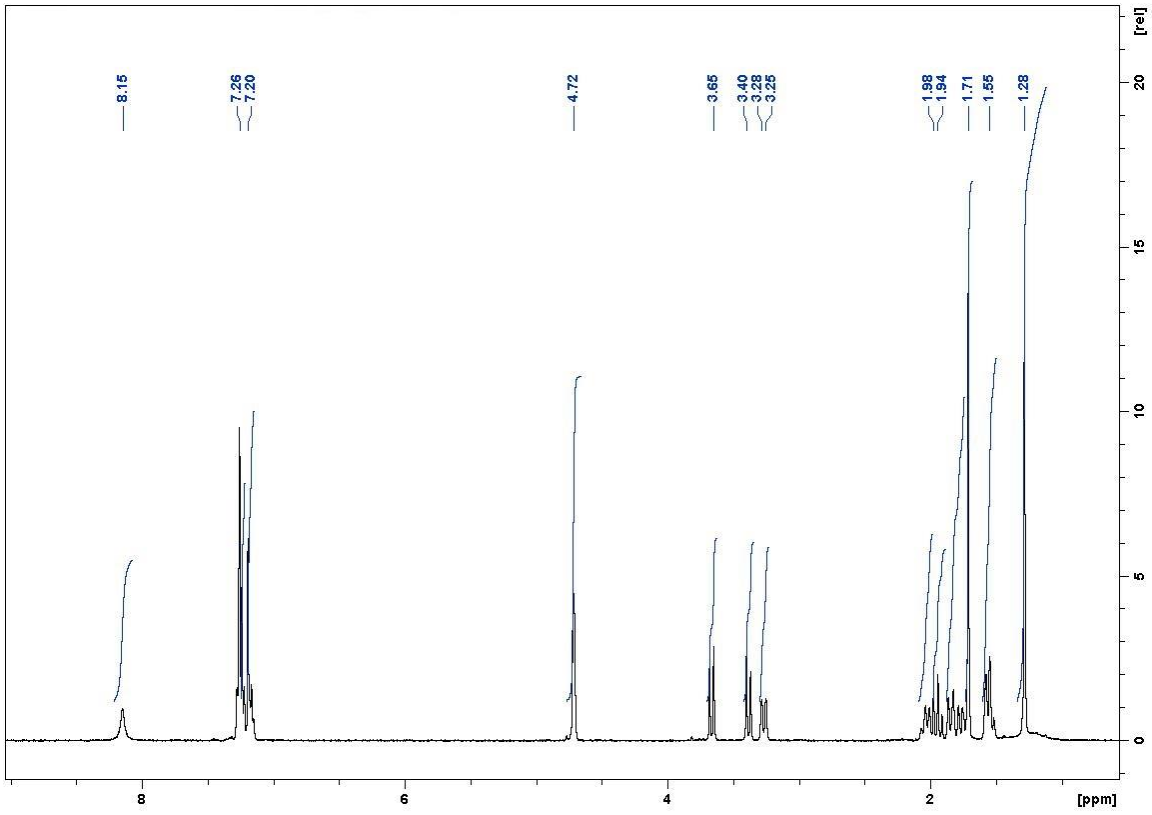

Figure S7. ^{1}H NMR spectrum of pure **1a-1** in $CDCl_3$ (re-dissolved crystals).

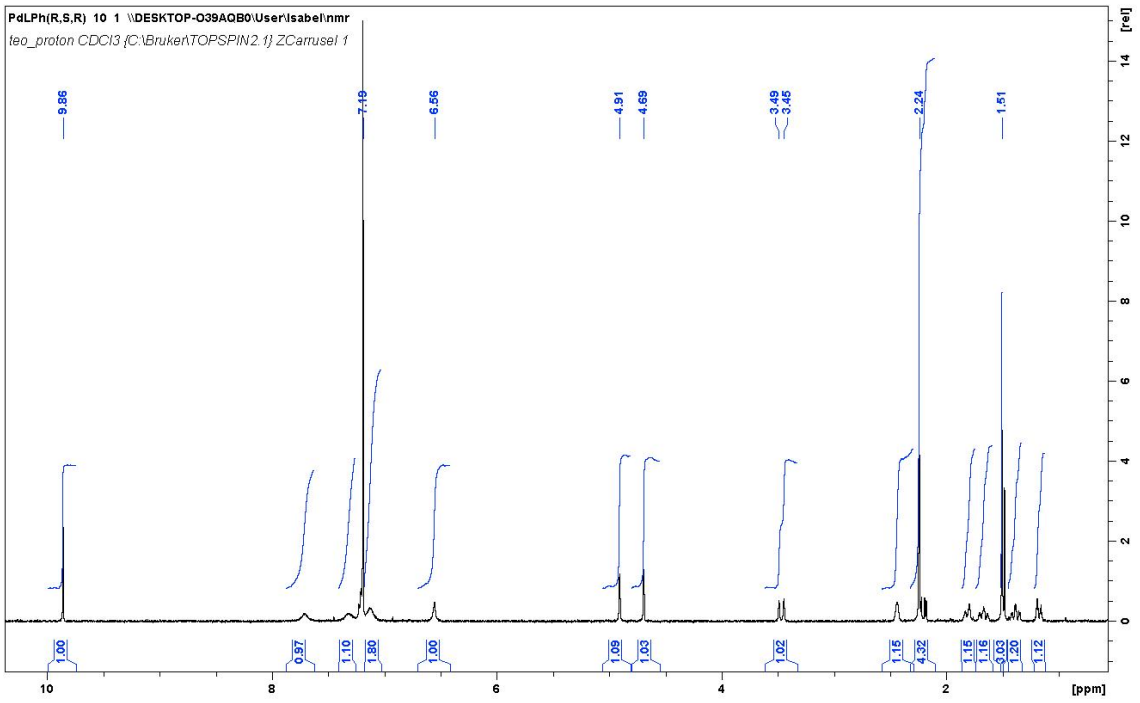

Figure S8. ^{1}H-^{15}N HMBC NMR spectrum of pure **1a-1** in $CDCl_3$ (re-dissolved crystals).

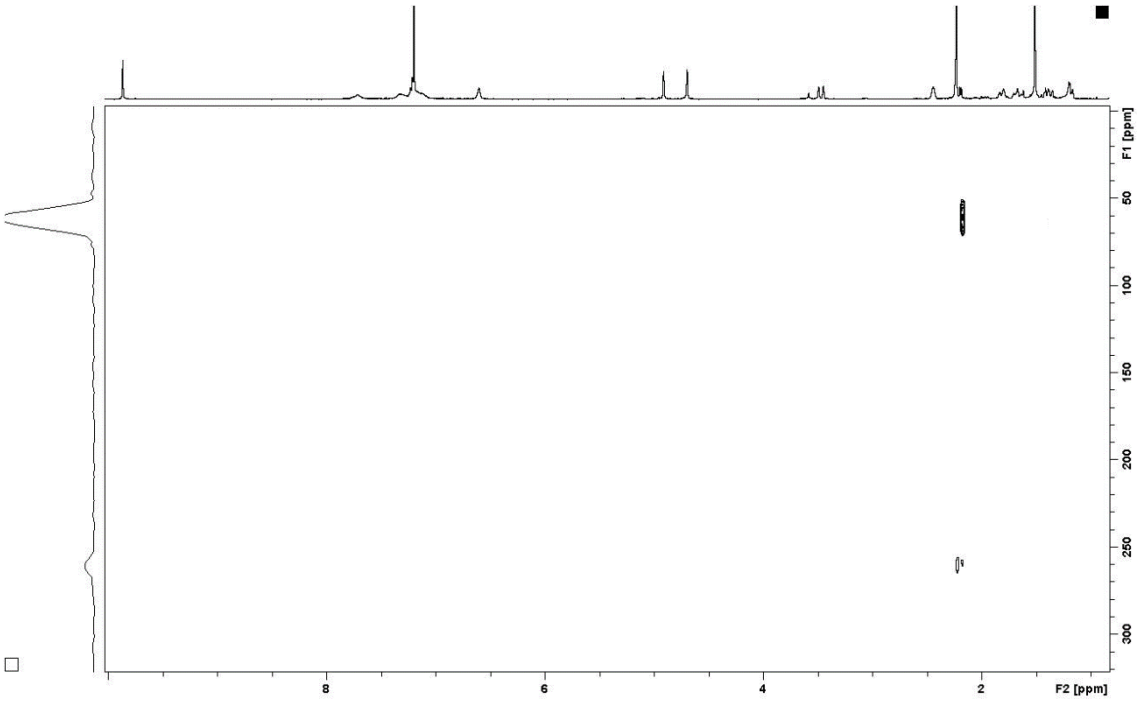

Figure S9. ^{13}C APT NMR spectrum of pure **1a-1** in $CDCl_3$ (re-dissolved crystals)

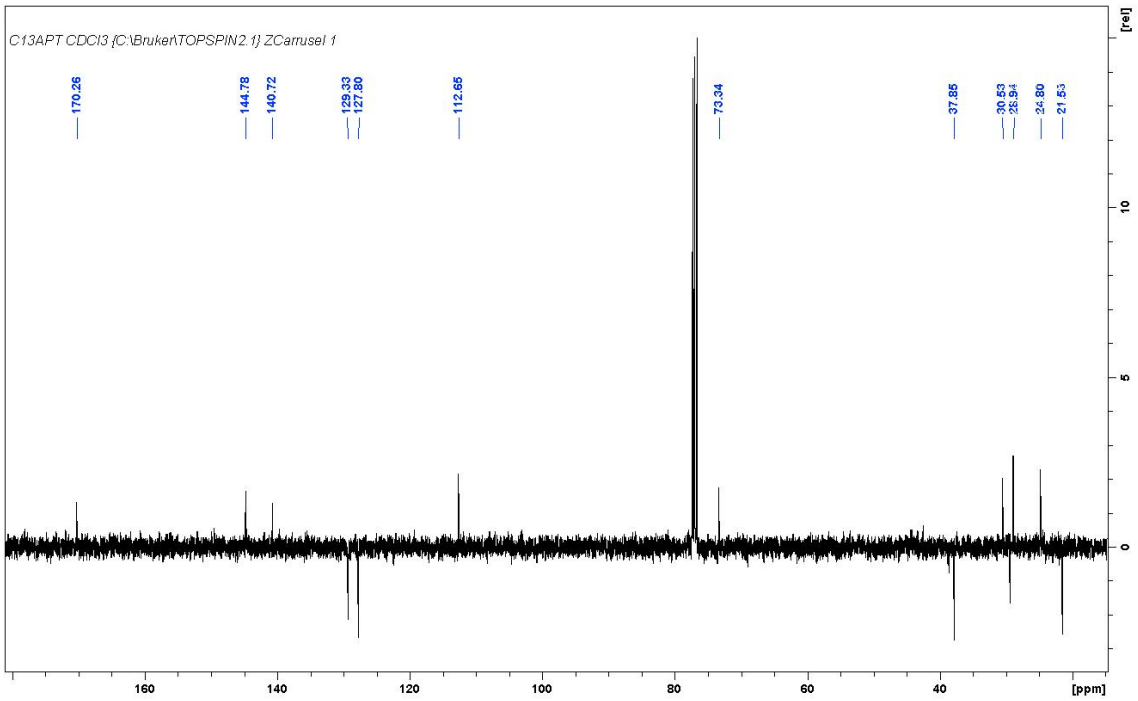

Figure S10. ^{1}H NMR spectrum of **1a-1** (major) +**1a-2** (minor) in $CDCl_3$ (crude solid obtained from synthetic reaction).

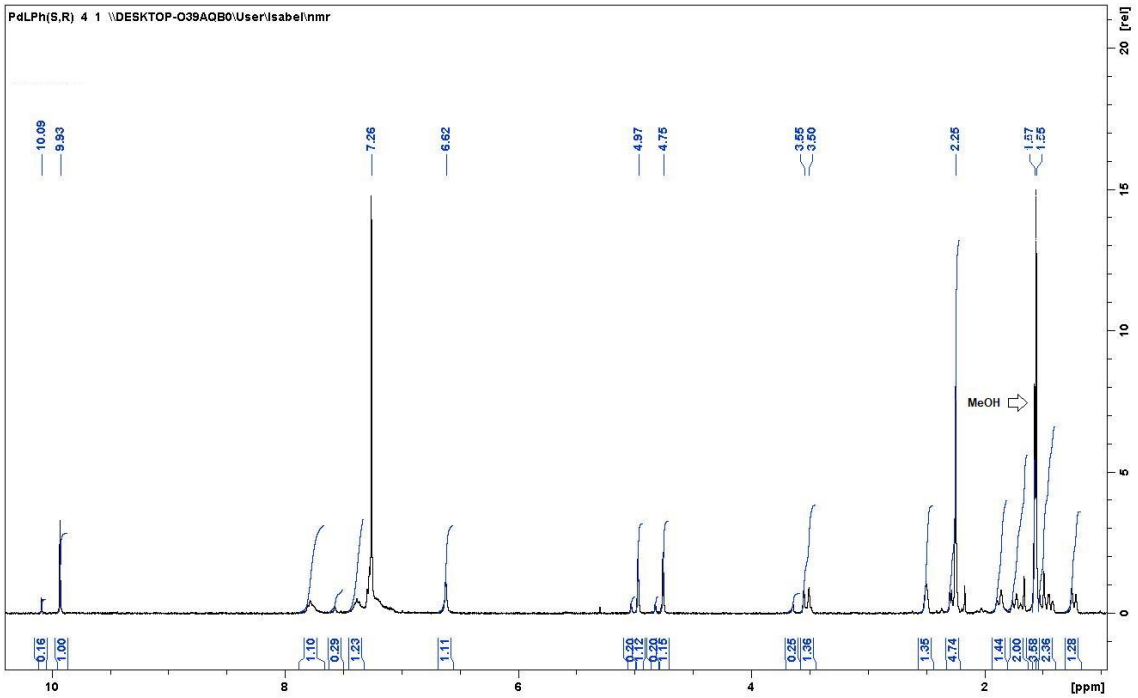

Figure S11. ^{1}H NMR spectrum of **1a'-1** (major) +**1a'-2** (minor) in $CDCl_3$ (crude solid obtained from synthetic reaction).

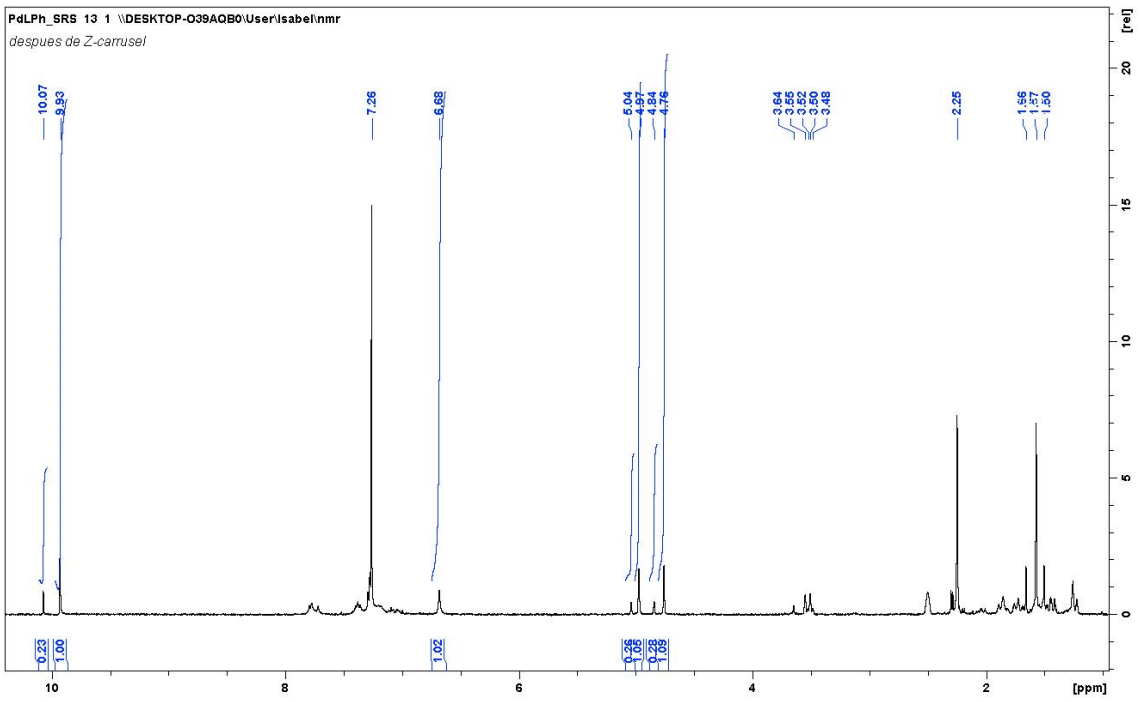

Figure S12. ^{1}H-^{15}N HMBC NMR spectrum of **1a-1** (major) +**1a-2** (minor) in $CDCl_3$ (crude solid obtained from the synthetic reaction), (full and expanded). Example of $\underline{CH_3}$CqNH and C$\underline{H_2}$(3) assignment.

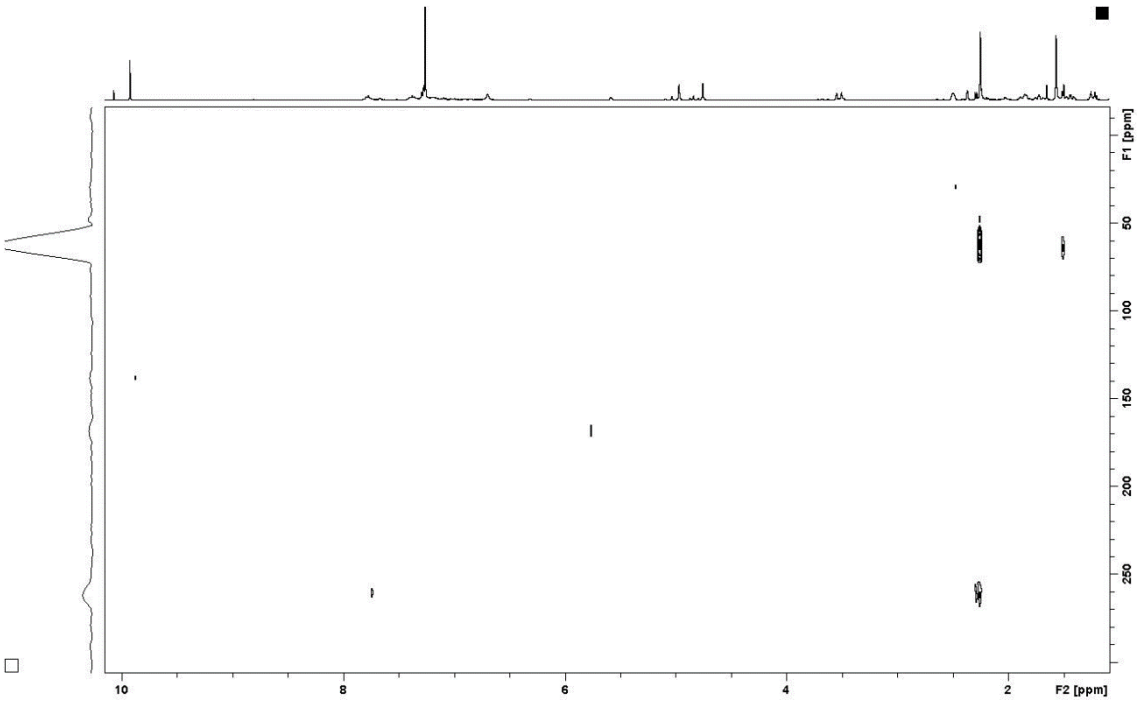

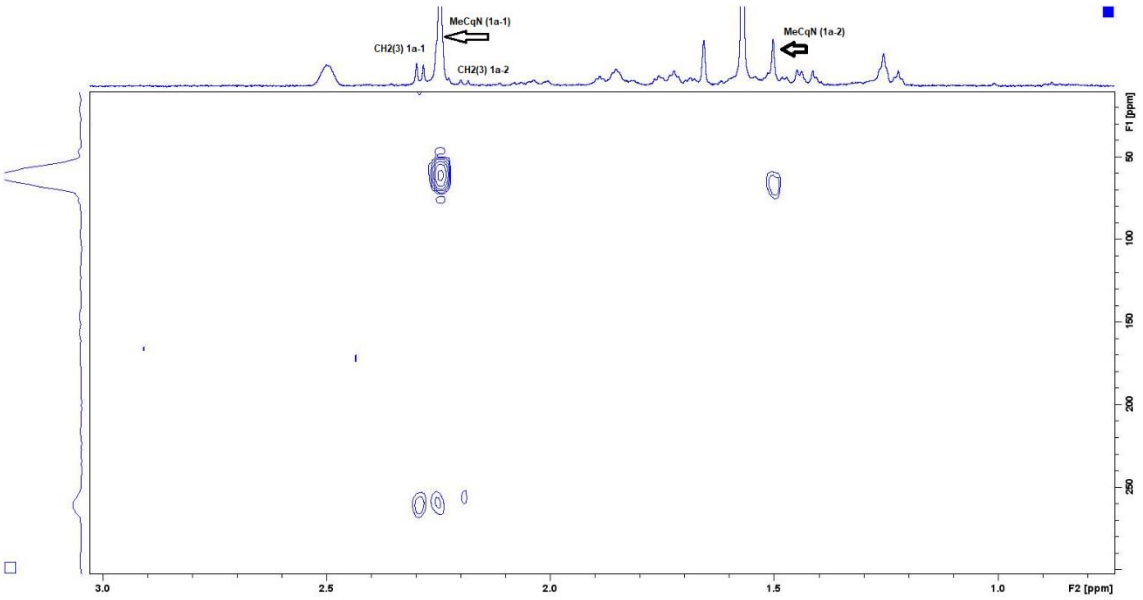

Figure S13. ^{13}C APT NMR spectrum of **1a-1** (major) +**1a-2** (minor) in $CDCl_3$ (crude solid obtained from synthetic reaction) (full and expanded).

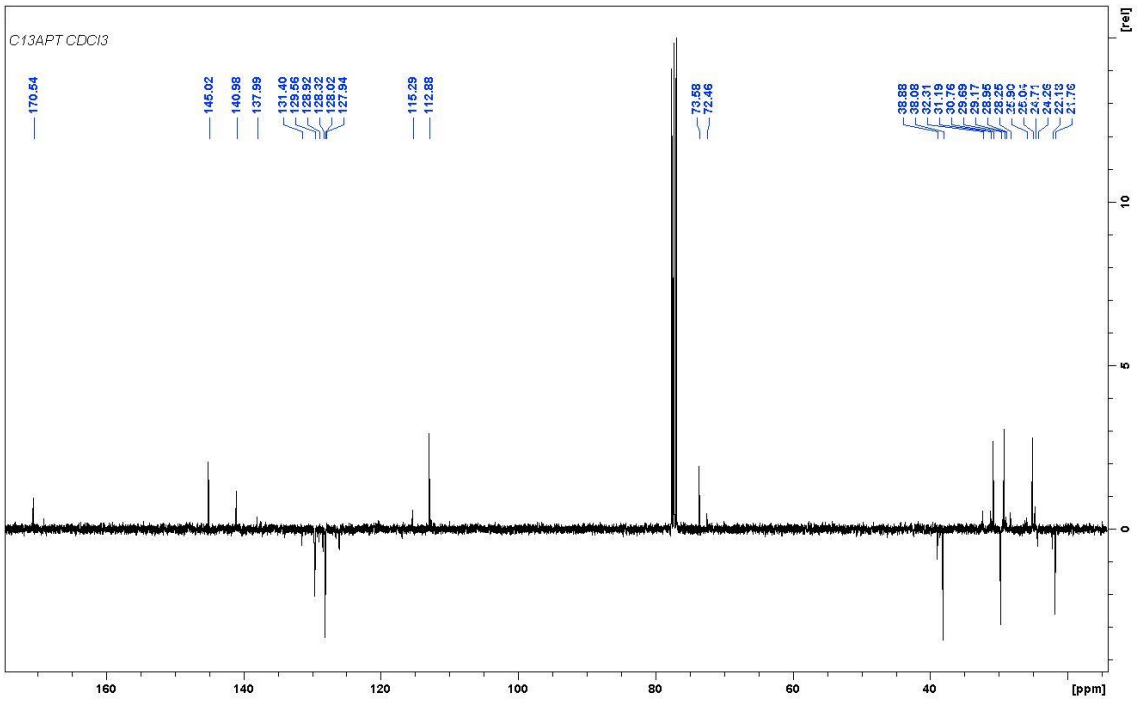

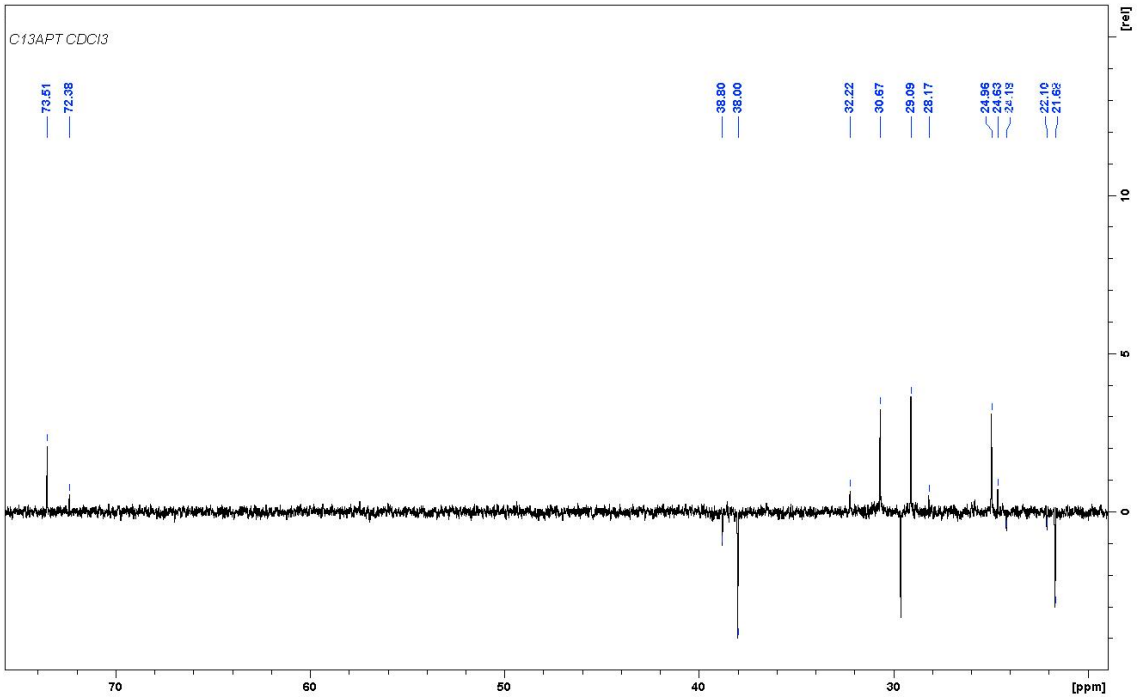

Figure S14. ^{1}H-^{13}C HSQC NMR spectrum of **1a-1** (major) +**1a-2** (minor) in $CDCl_3$ (crude solid obtained from synthetic reaction).

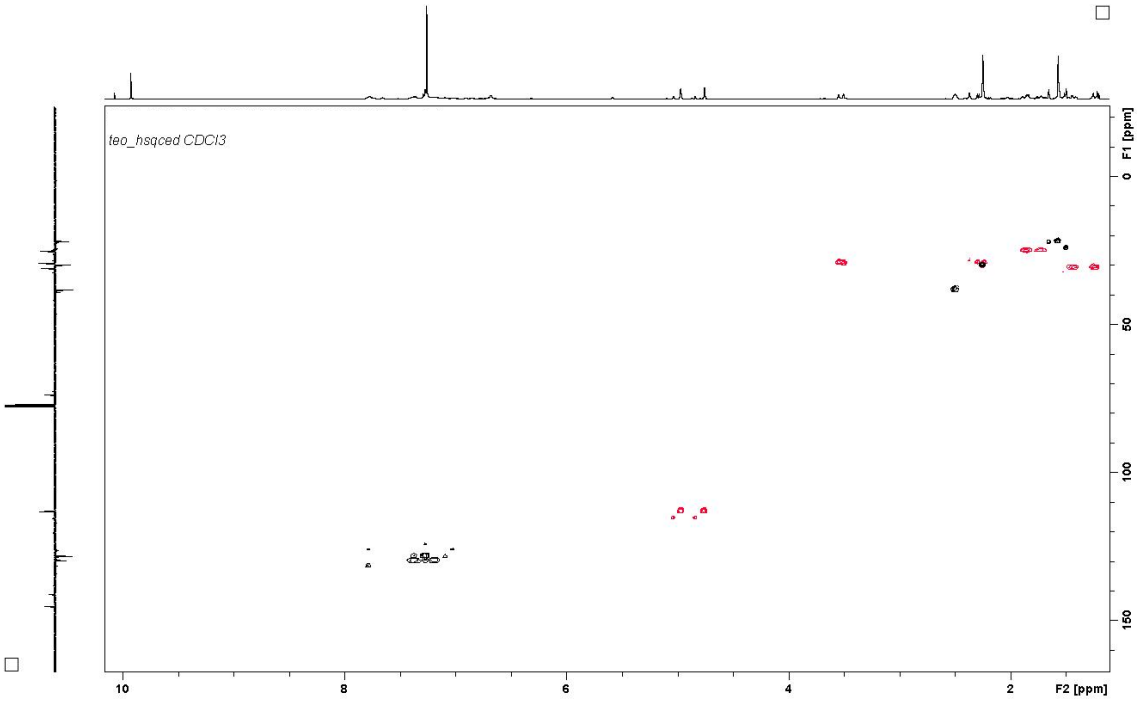

Figure S15. ^{1}H-^{1}H NOESY NMR spectrum of **1a-1** (major) +**1a-2** (minor) in $CDCl_3$ (crude solid obtained from the synthesis reaction).

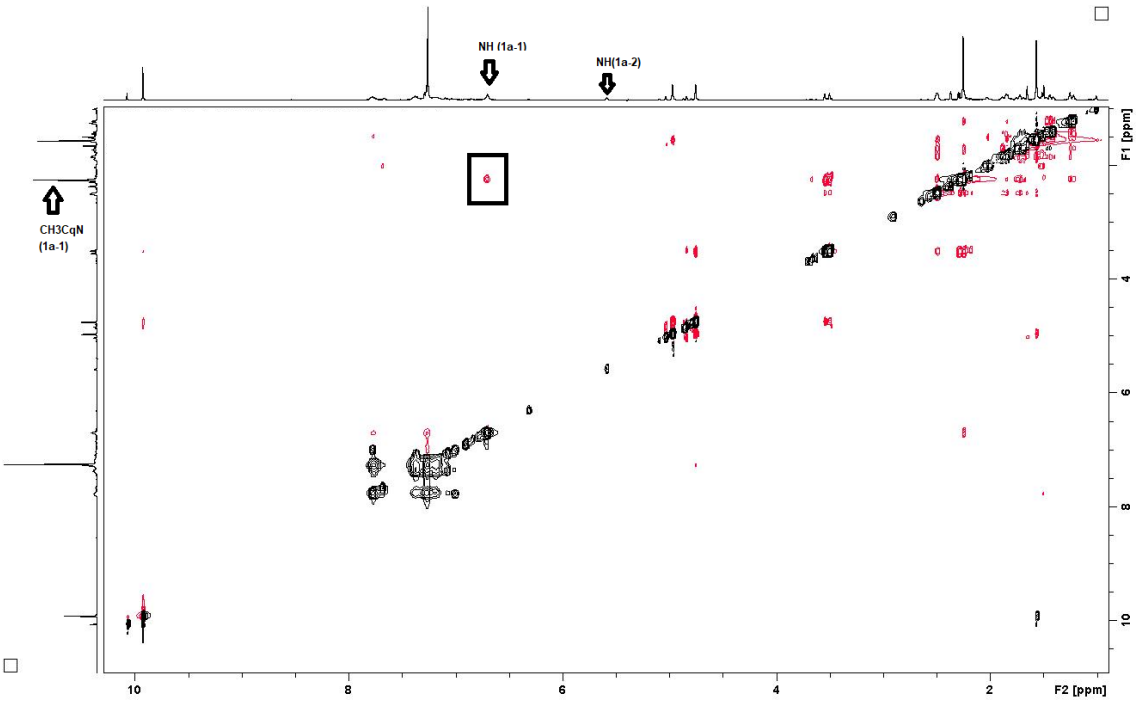

Figure S16. ^{1}H NMR spectrum of **1b-1** (minor) +**1b-2** (major) in $CDCl_3$.

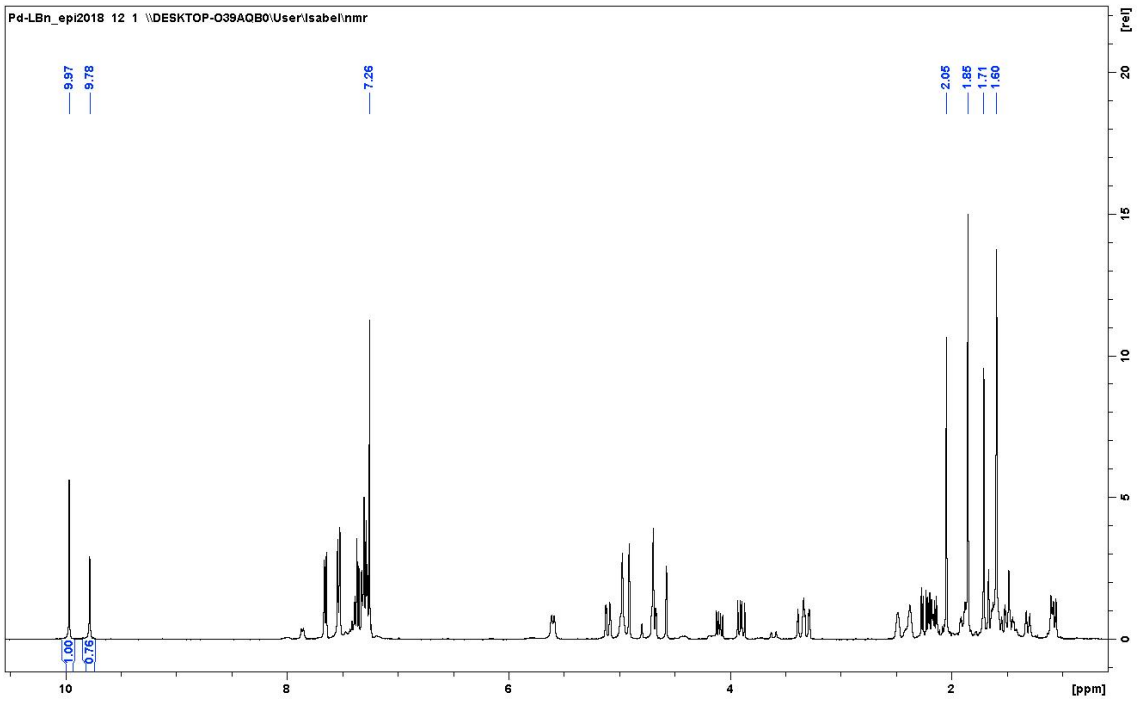

Figure S17. ^{1}H NMR spectrum of **1b'-1** (minor) +**1b'-2** (major) in $CDCl_3$.

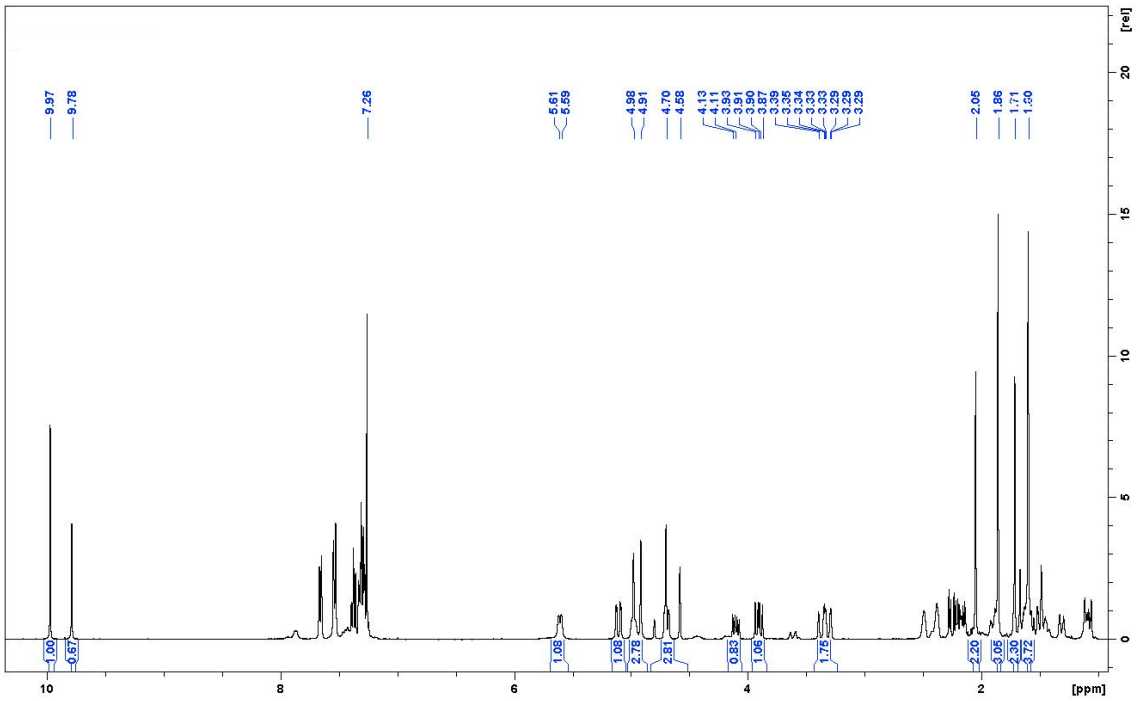

Figure S18. ^{1}H-^{15}N HMBC NMR spectrum of **1b-1** (minor) +**1b-2** (major) in $CDCl_3$.

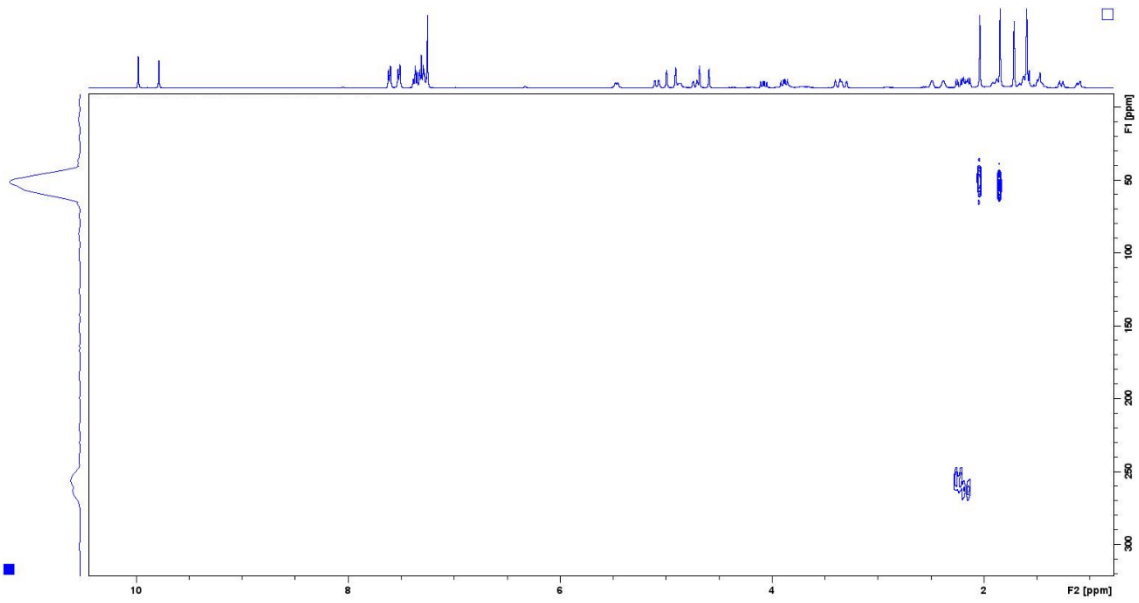

Figure S19. ^{1}H-^{13}C HSQC NMR spectrum of **1b-1** (minor) +**1b-2** (major) in $CDCl_3$.

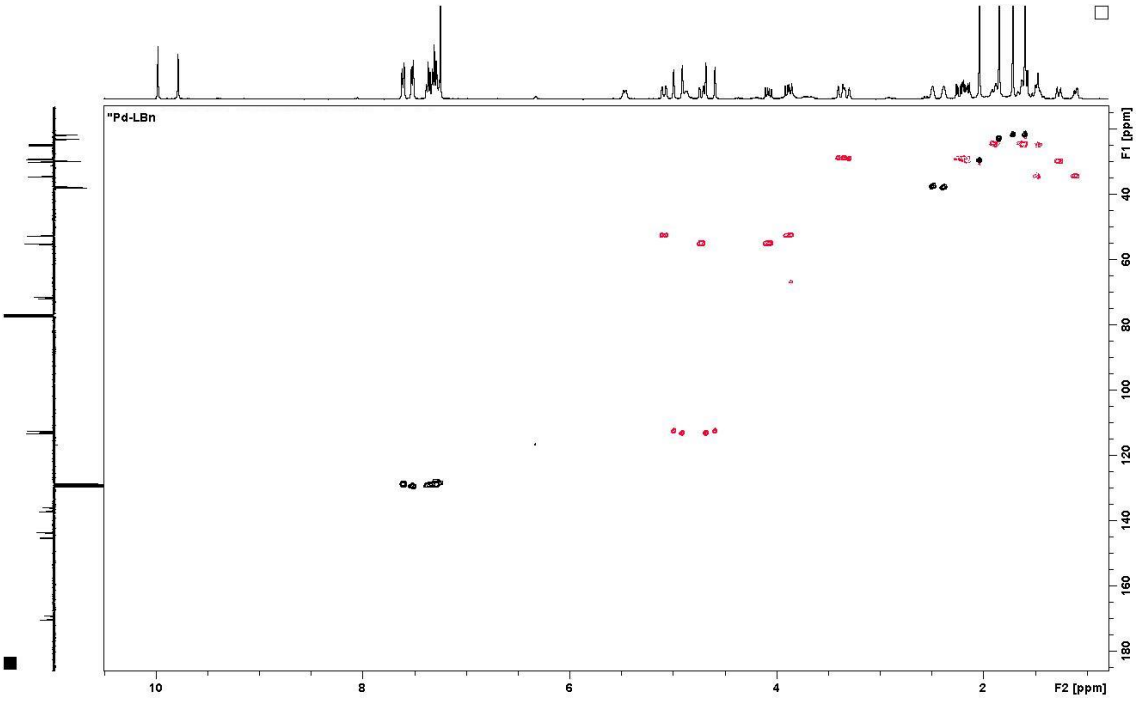

Figure S20. ^{1}H-^{13}C HMBC NMR spectrum of **1b-1** (minor) +**1b-2** (major) in $CDCl_3$. Example of NOH and CH_2(6) assignment.

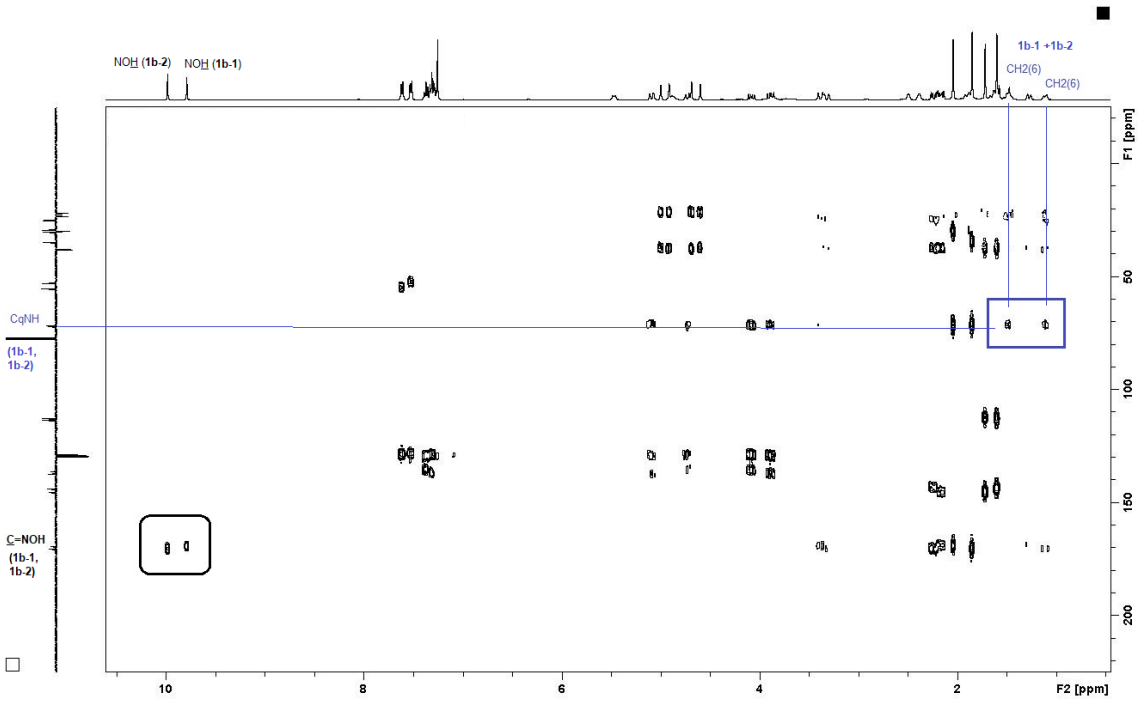

Figure S21. ^{1}H-^{1}H COSY NMR spectrum of **1b-1** (minor) +**1b-2** (major) in $CDCl_3$ (example of NH assignment)

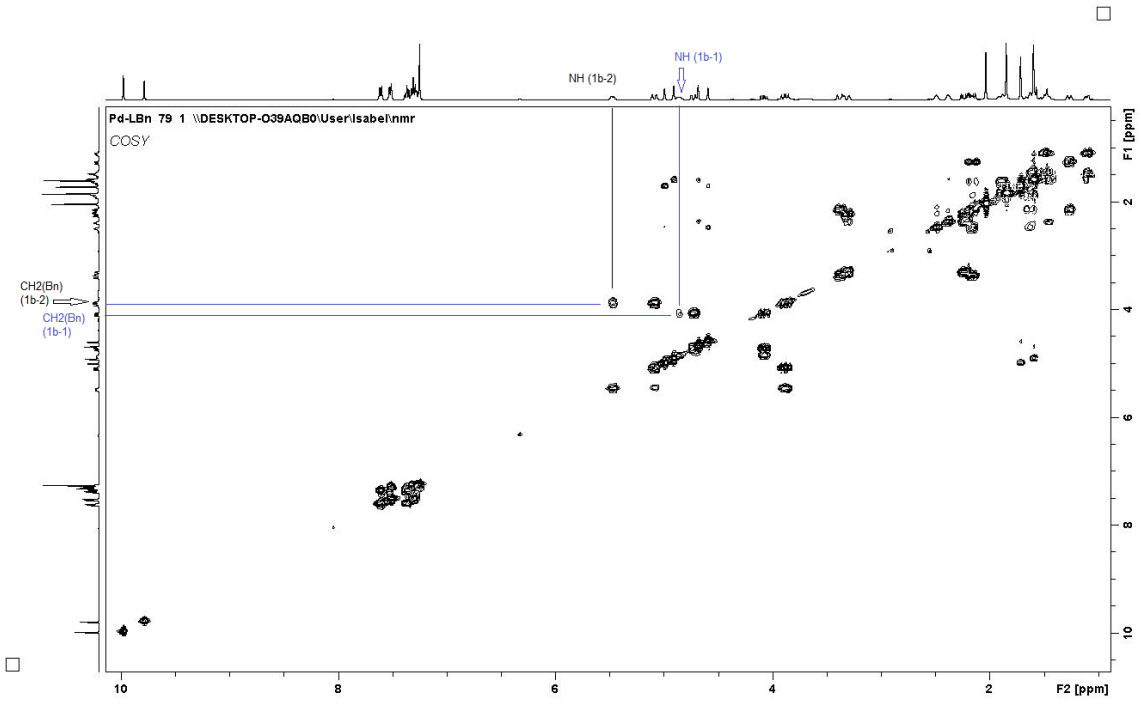

Figure S22. ^{1}H-^{1}H NOESY NMR spectrum of **1b-1** (minor) +**1b-2** (major) in $CDCl_3$ (full and expanded)

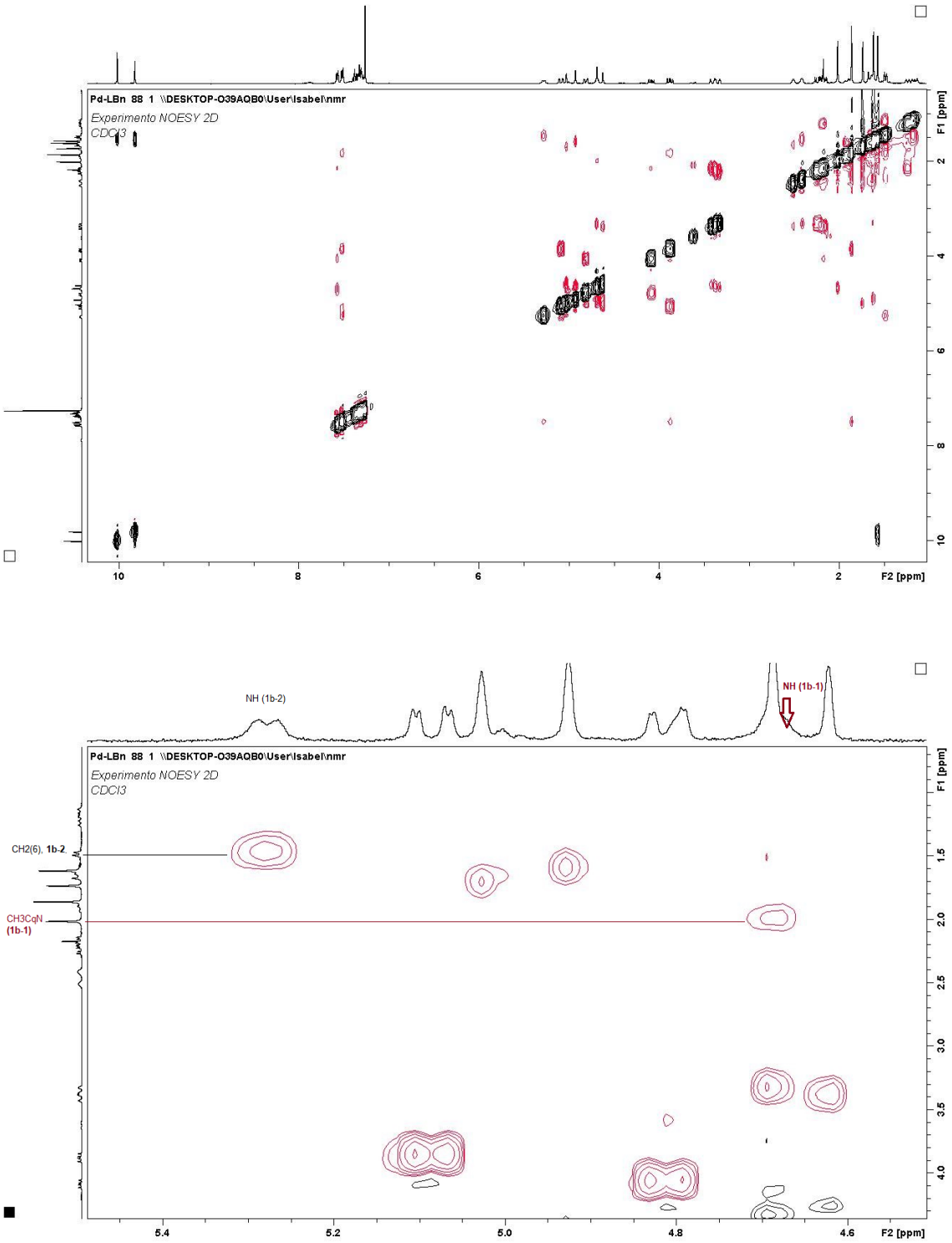

Figure S23. ^{1}H NMR spectrum of **2a** in $CDCl_3$.

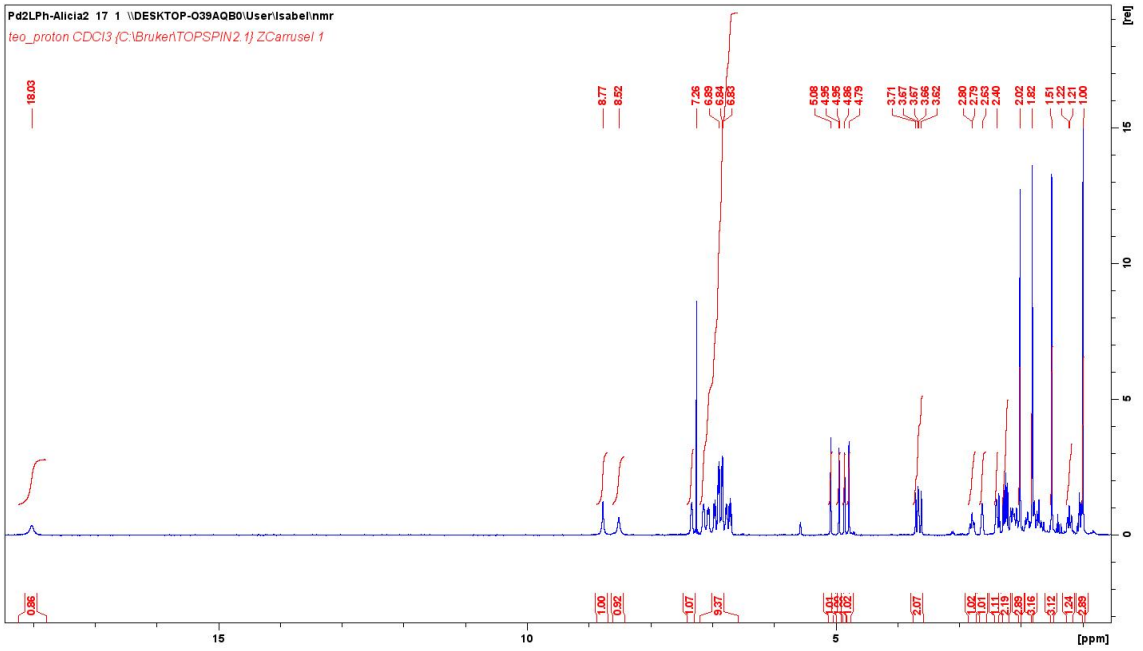

Figure S24. ^{1}H NMR spectrum of **2a'** in $CDCl_3$.

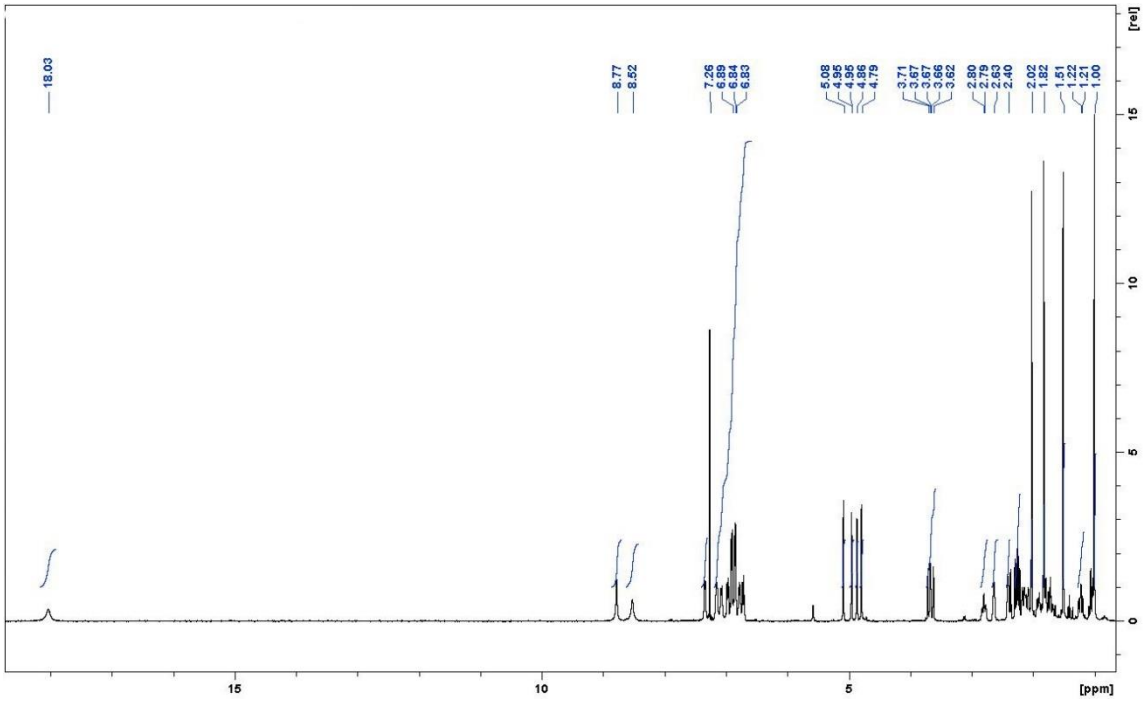

Figure S25. ^{13}C APT NMR spectrum of **2a** in $CDCl_3$.

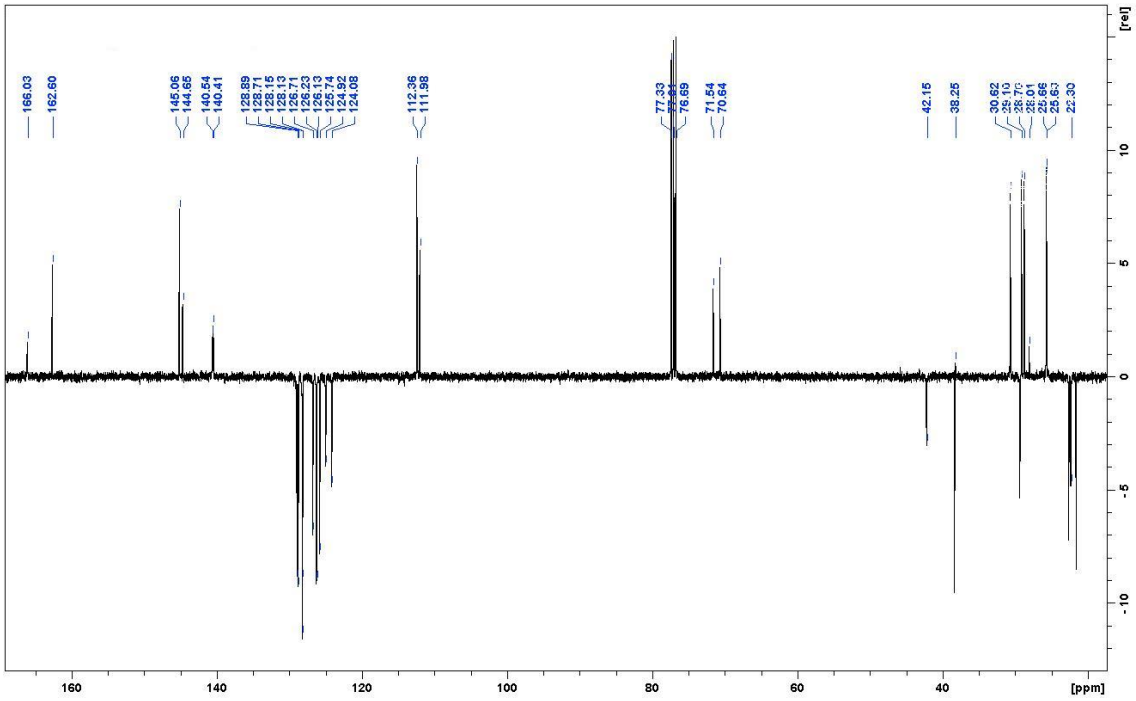

Figure S26. ^{13}C-^{1}H HSQC NMR spectrum of **2a** in $CDCl_3$.

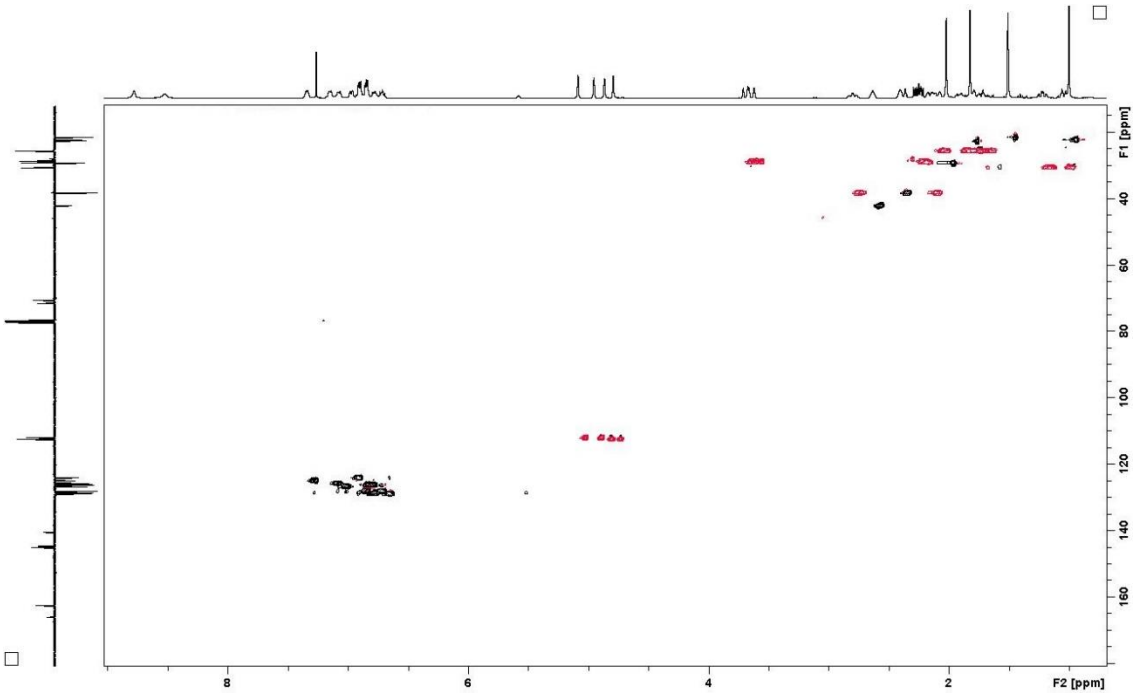

Figure S27. ^{15}N-^{1}H HMBC NMR spectrum of **2a** in $CDCl_3$.

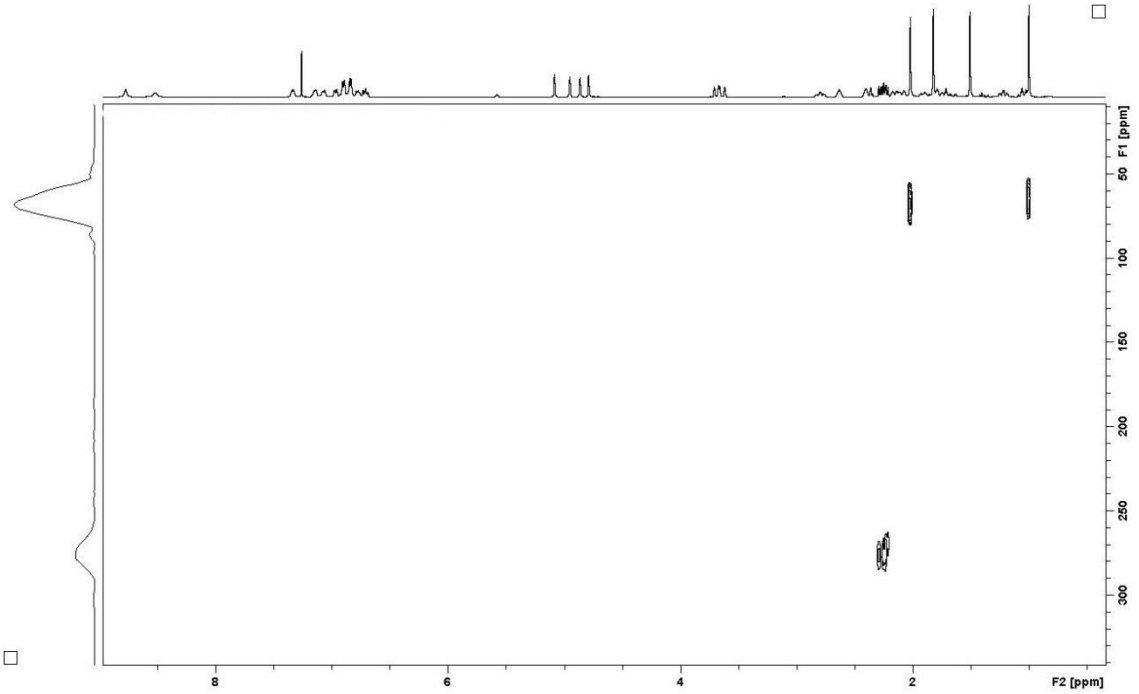

Figure S28. ^{1}H-^{1}H COSY NMR spectrum of **2a** in $CDCl_3$.

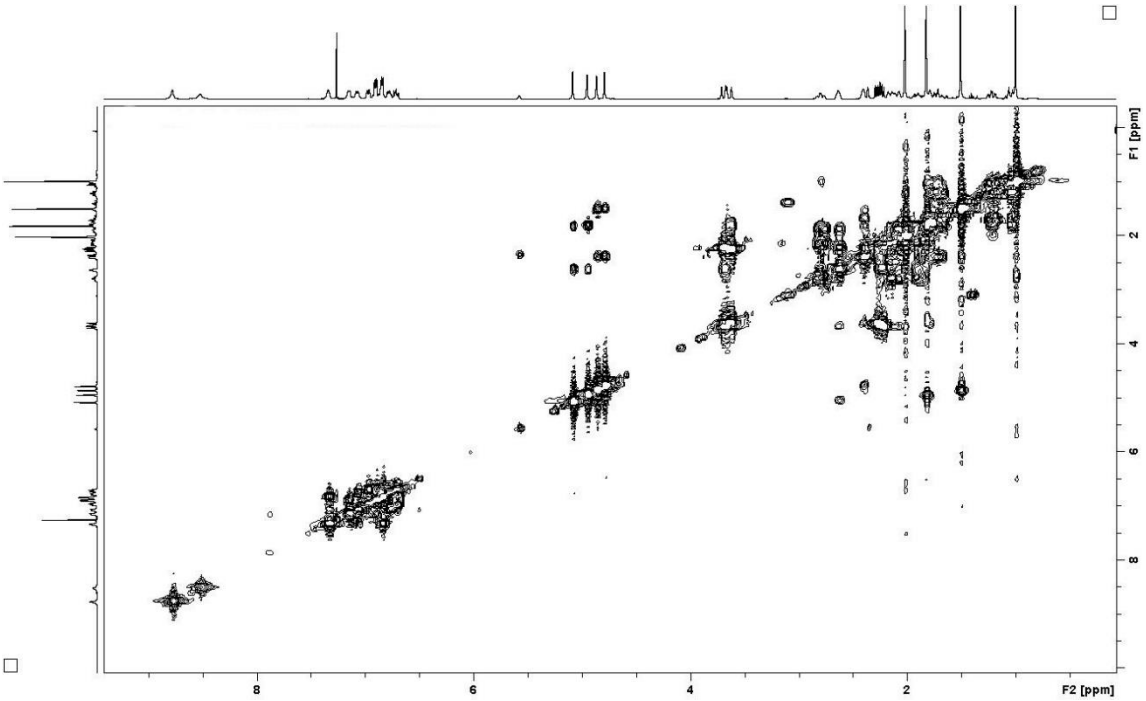

Figure S29. 2D NOESY NMR spectrum of **2a** in $CDCl_3$

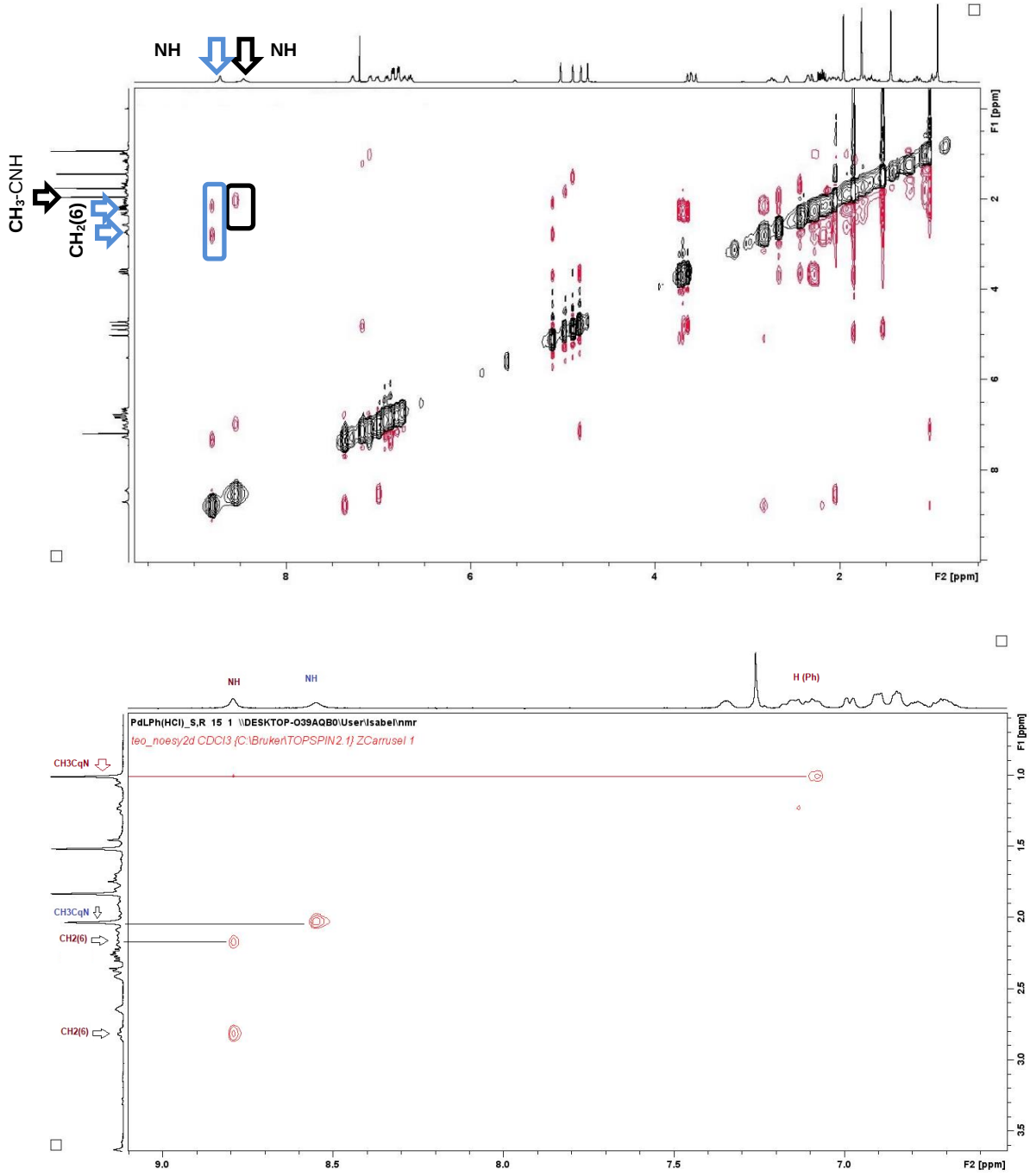

Figure S30. ^{1}H NMR spectrum of **2b-1** (major) + **2b-2** (minor) in $CDCl_3$.

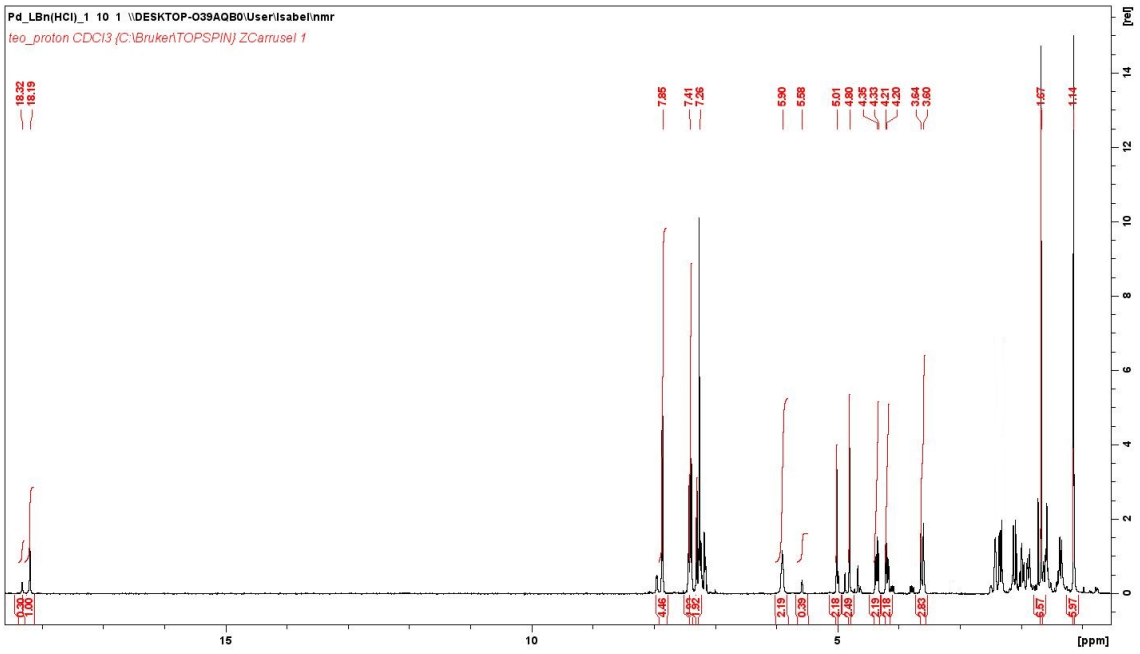

Figure S31. ^{1}H NMR spectrum of **2b'-1** (major) + **2b'-2** (minor) in $CDCl_3$.

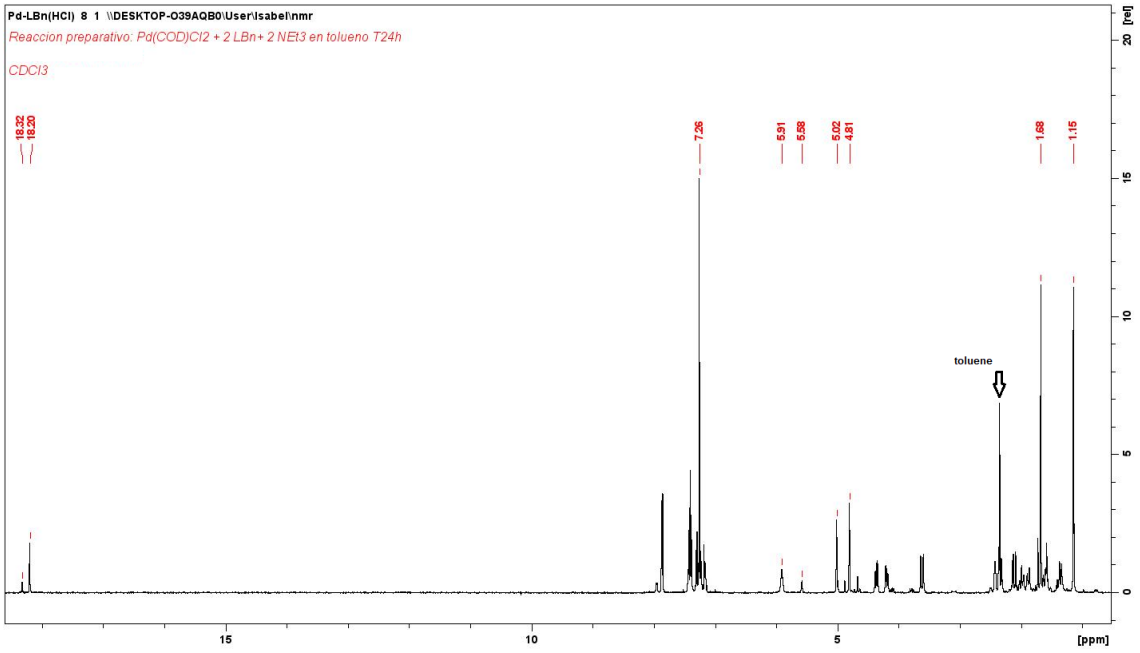

Figure S32. ^{13}C APT NMR spectrum of **2b-1** (major) + **2b-2** (minor) in $CDCl_3$ (full and expanded)

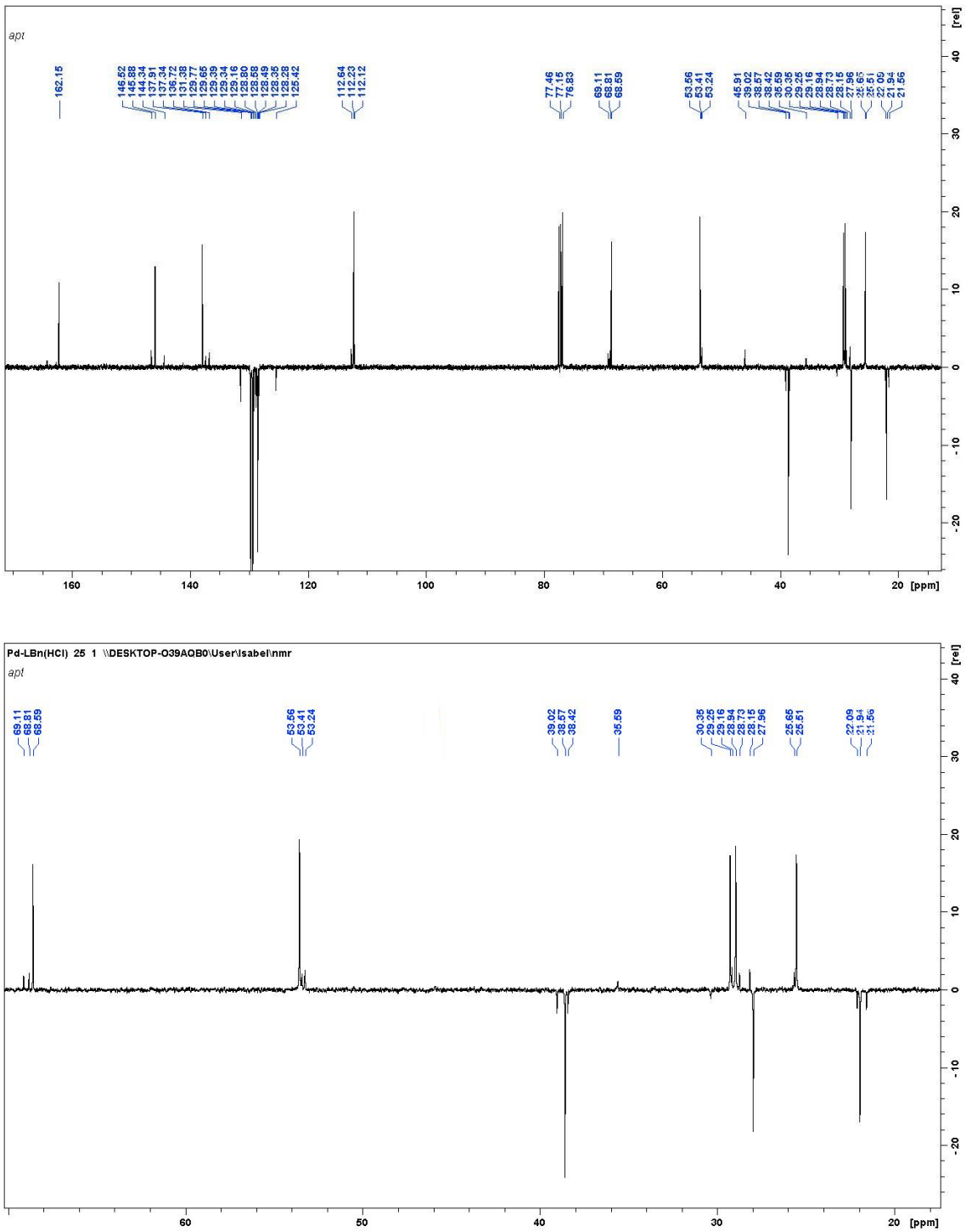

Figure S33. ^{1}H ^{13}C HSQC NMR spectrum of **2b-1** (major) + **2b-2** (minor) in $CDCl_3$ (full and expanded)

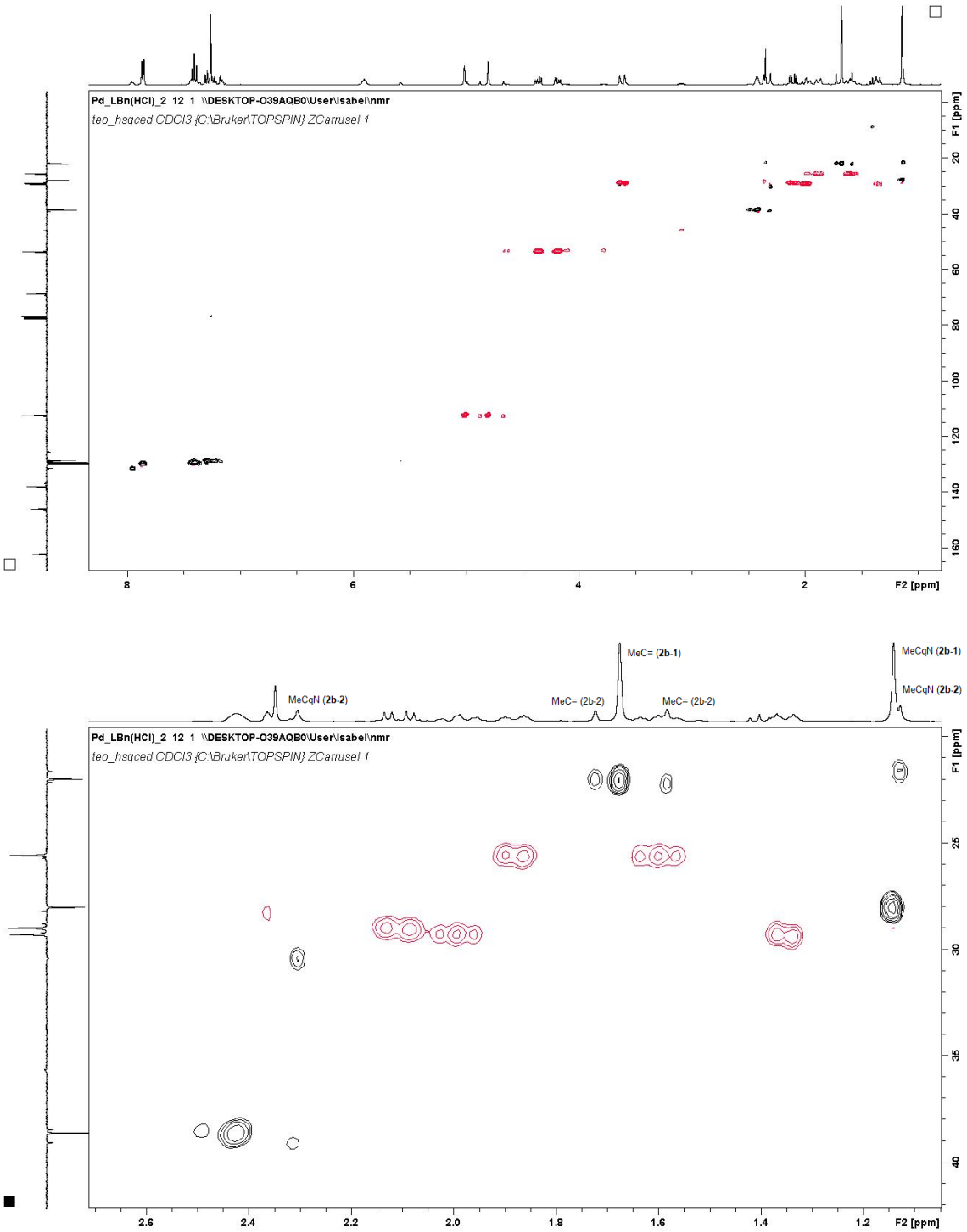

Figure S34. ^{13}C-^{1}H HMBC NMR spectrum of **2b-1** (major) + **2b-2** (minor) in $CDCl_3$.

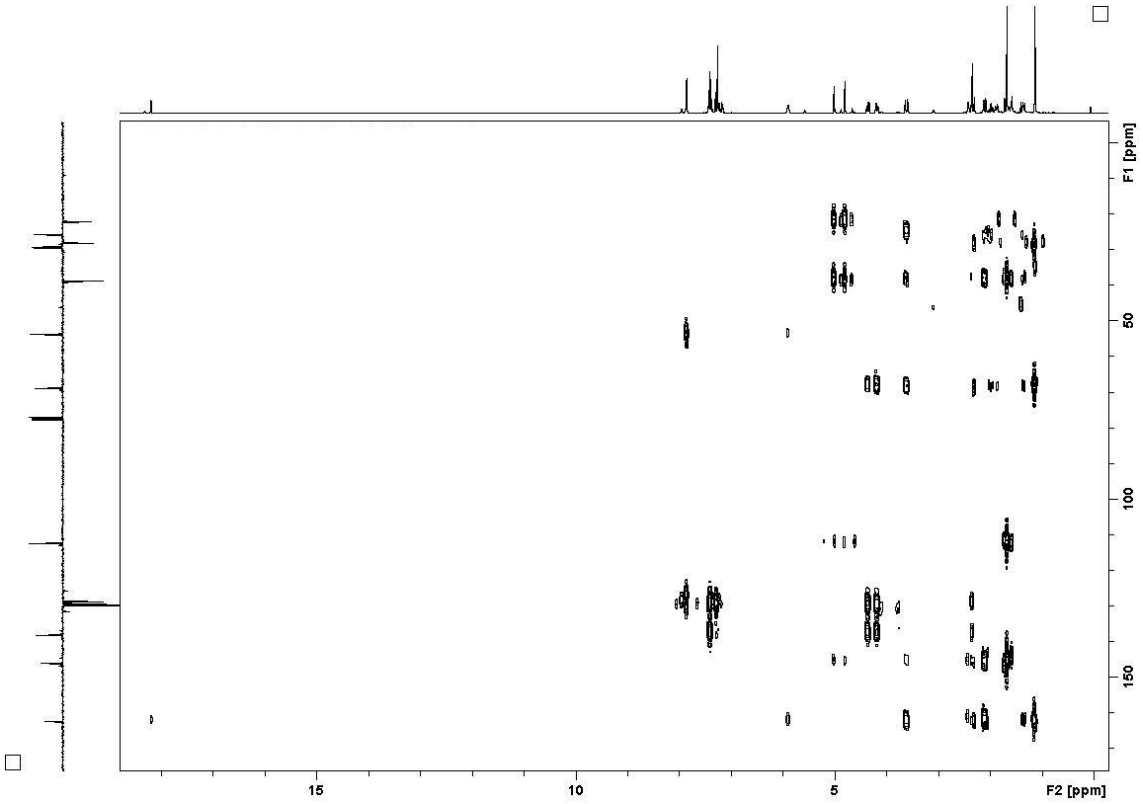

Figure S35. ^{15}N-^{1}H HMBC NMR spectrum of **2b-1** (major) + **2b-2** (minor) in $CDCl_3$ (full and expanded)

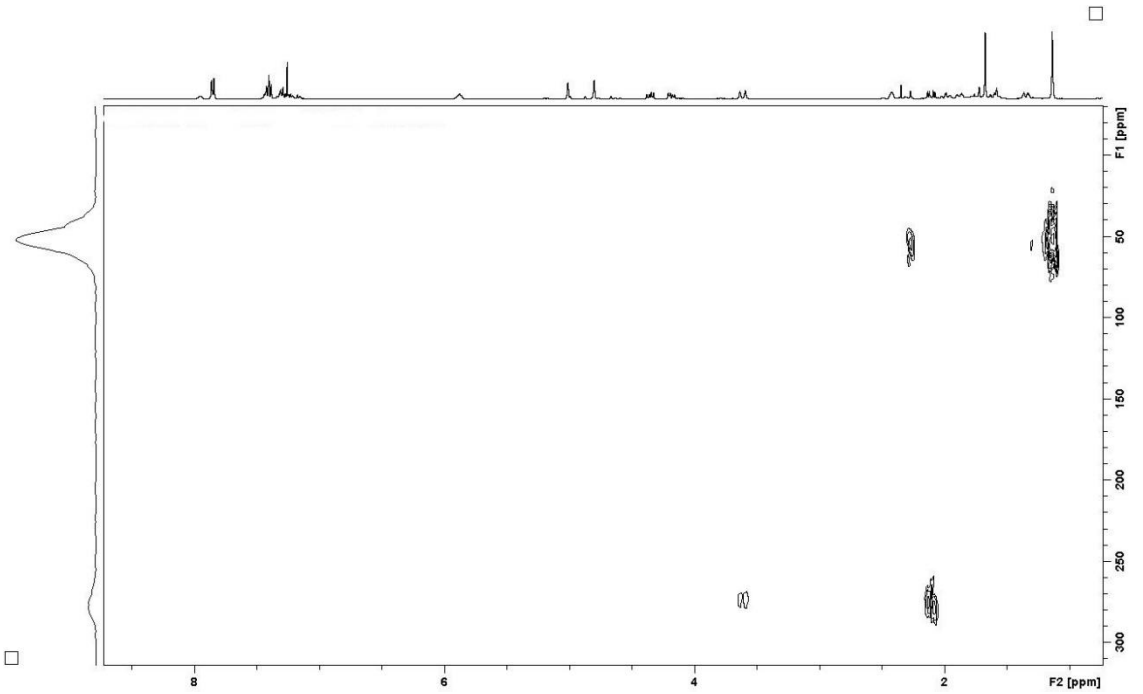

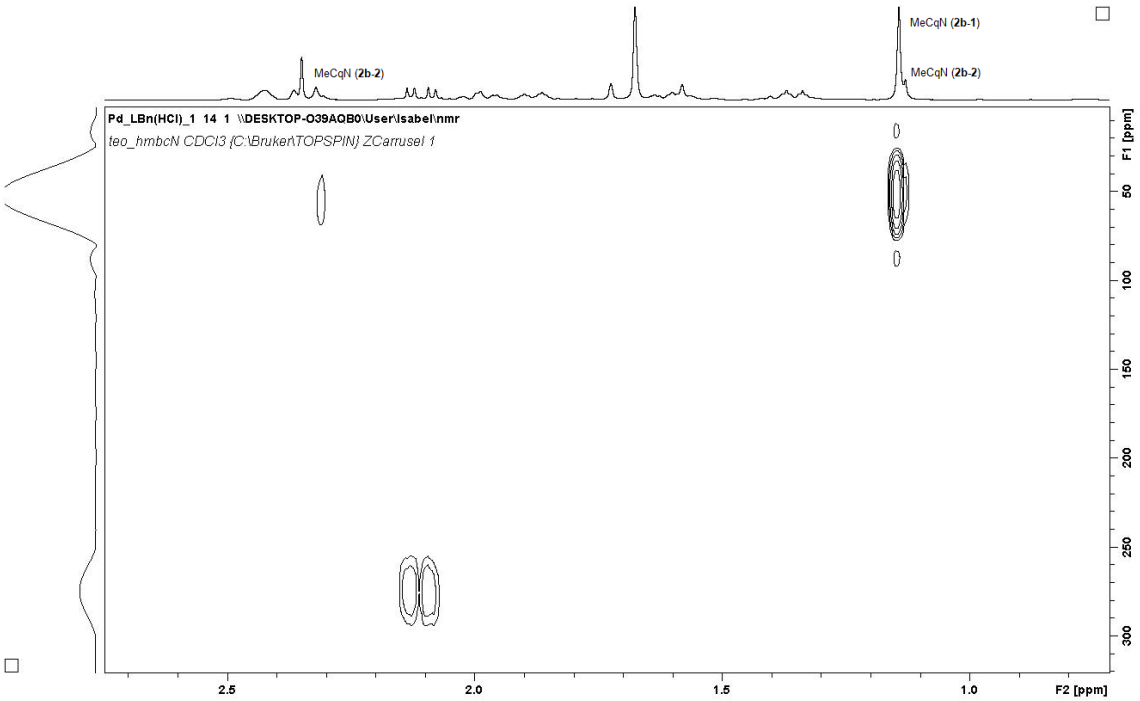

Figure S36. ^{1}H-^{1}H COSY NMR spectrum of **2b-1** (major) + **2b-2** (minor) in $CDCl_3$.

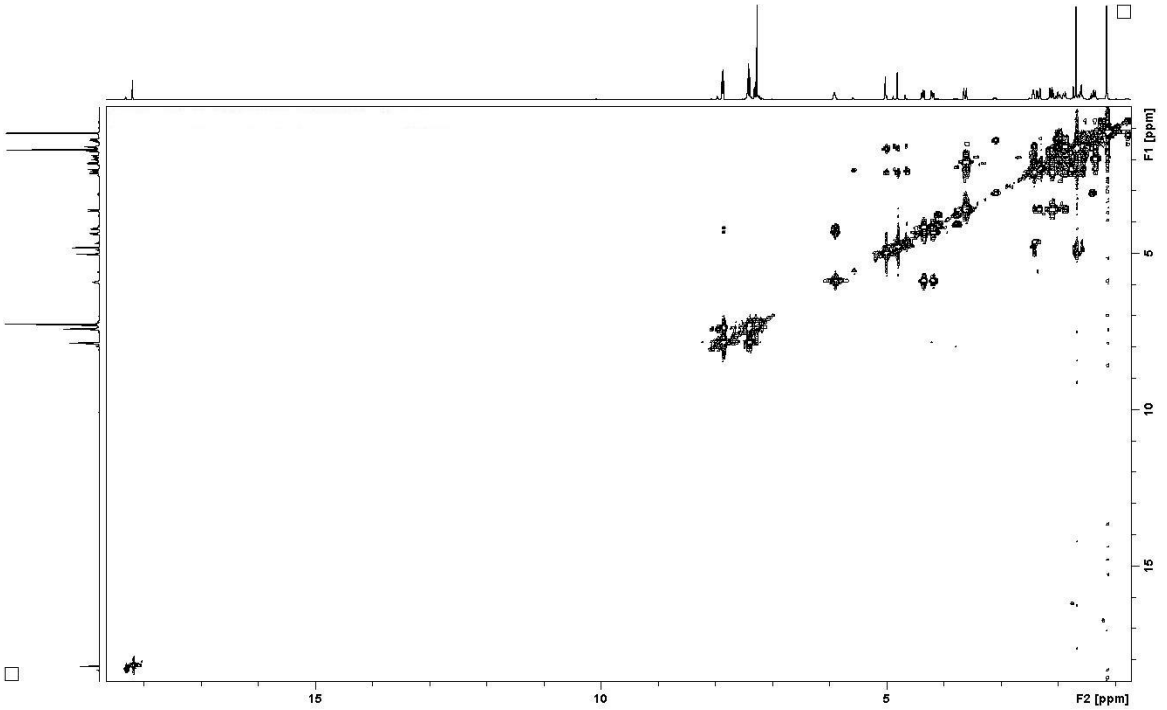

Figure S37. 2D NOESY NMR spectrum of **2b-1** (major) + **2b-2** (minor) in $CDCl_3$.

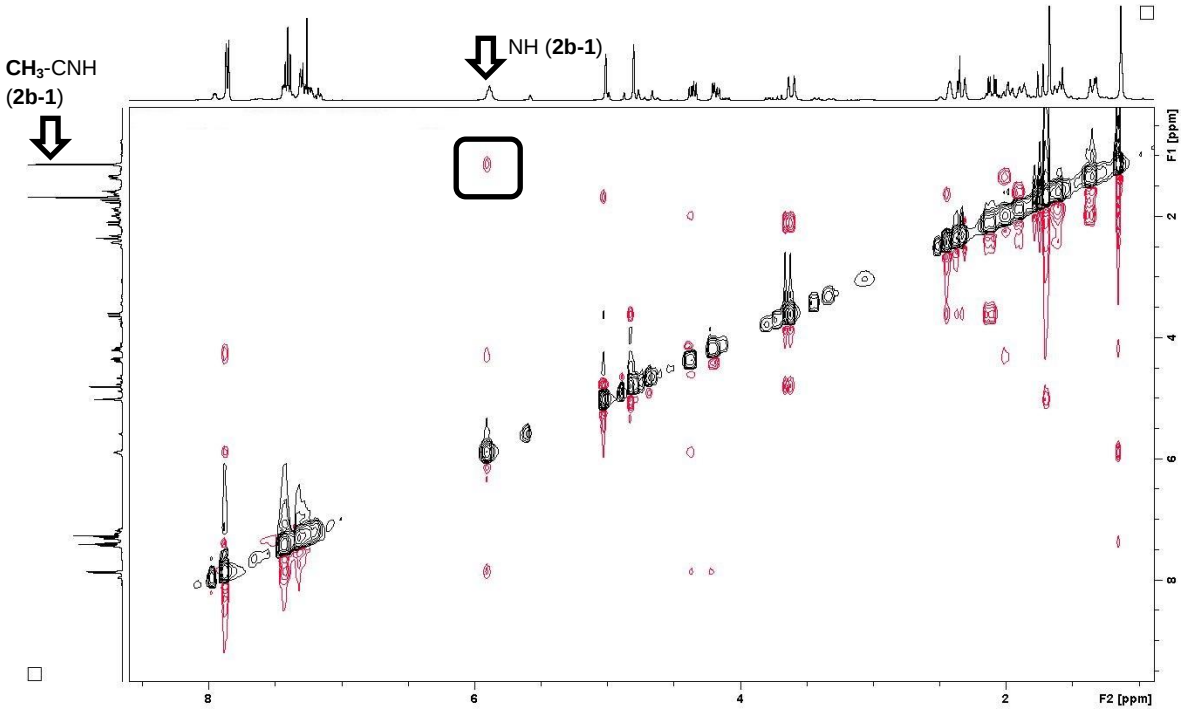

Figure S38. Time-dependent ^{1}H NMR spectra of **2b-1** (minor) + **2b-2** (major) (5 mM) in water-d_2 (pH* = 7.3).

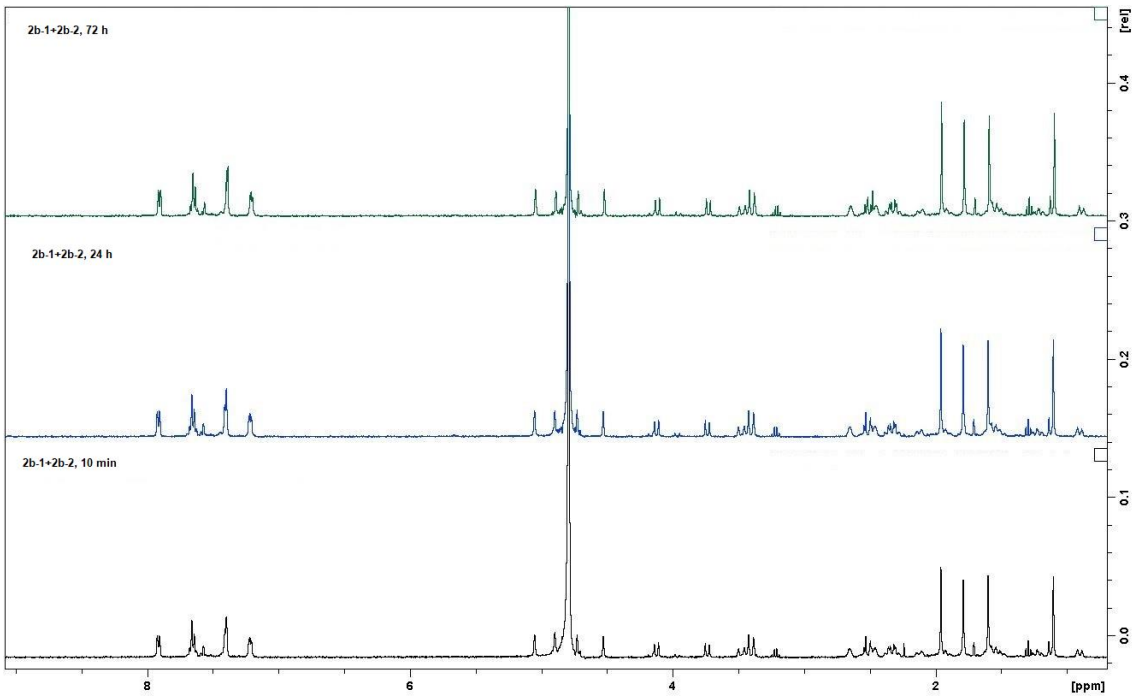

Figure S39. ^{1}H NMR spectrum of **2b-1** (minor) + **2b-2** (major) in water-d_2.

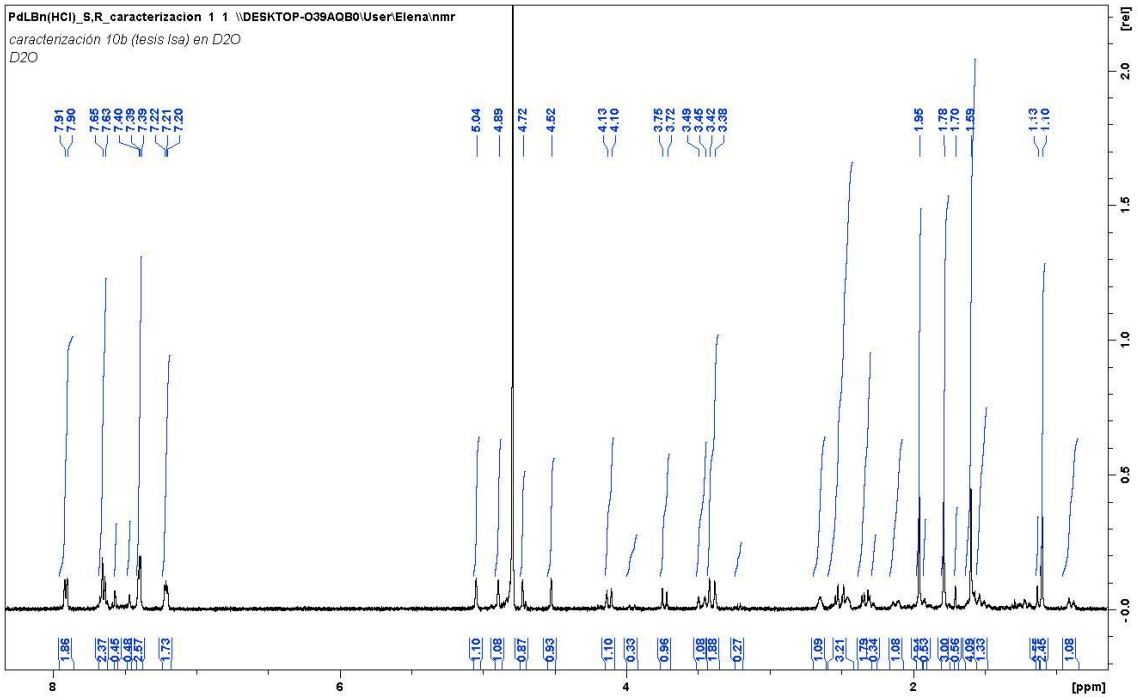

Figure S40. ^{1}H NMR spectrum of **2b-1** (*minor)* + **2b-2** (major) in methanol-d_4.

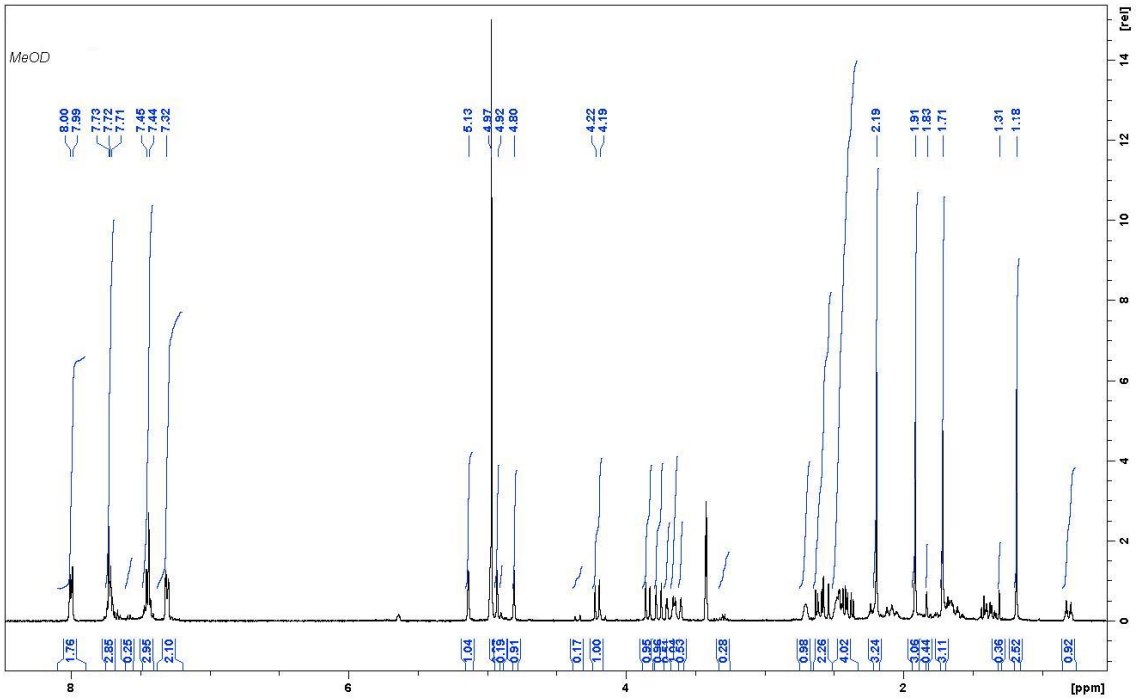

Figure S41. ^{13}C APT NMR spectrum of **2b-1** (*minor)* + **2b-2** (major) in water-d_2.

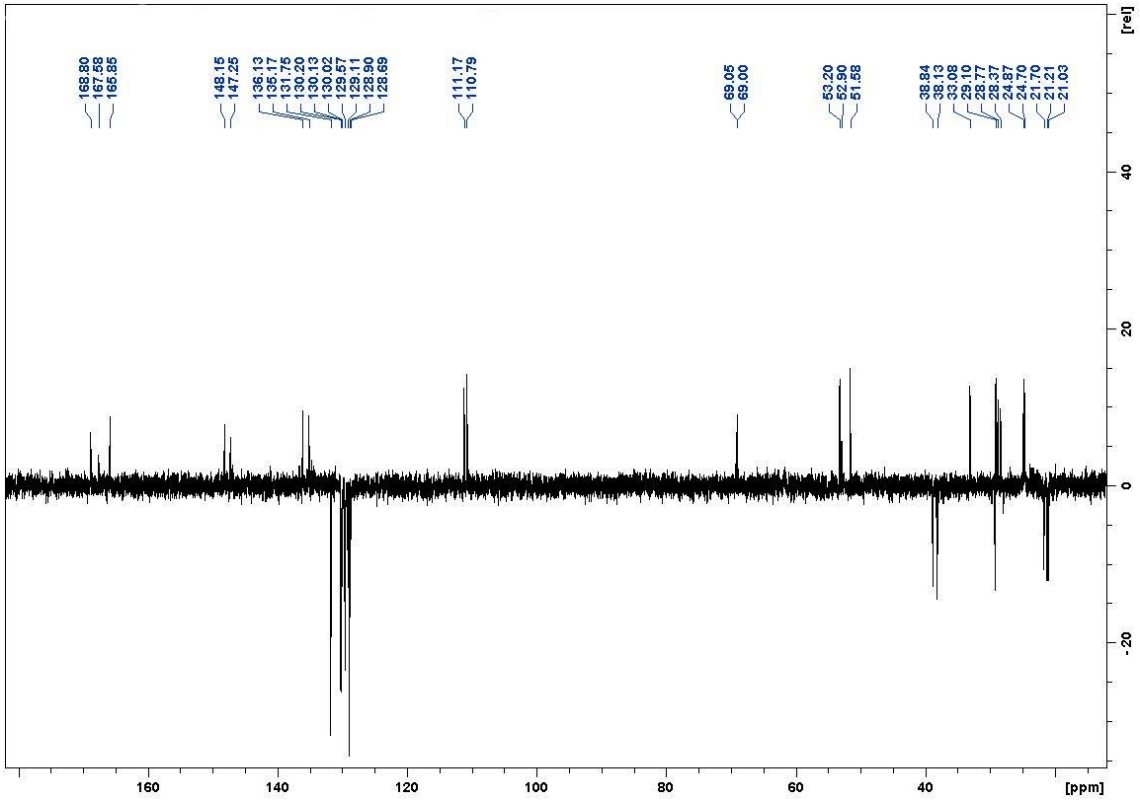

Figure S42. ^{13}C-^{1}H HSQC NMR spectrum of **2b-1** (*minor)* + **2b-2** (major) in water-d_2 (full and expanded)

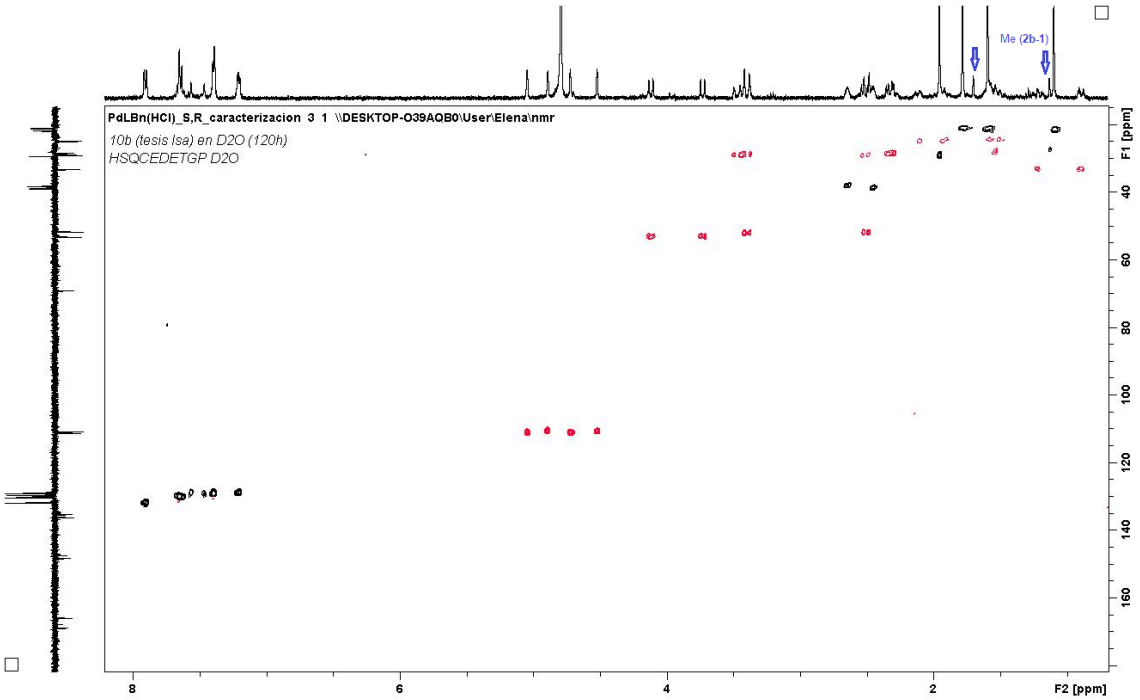

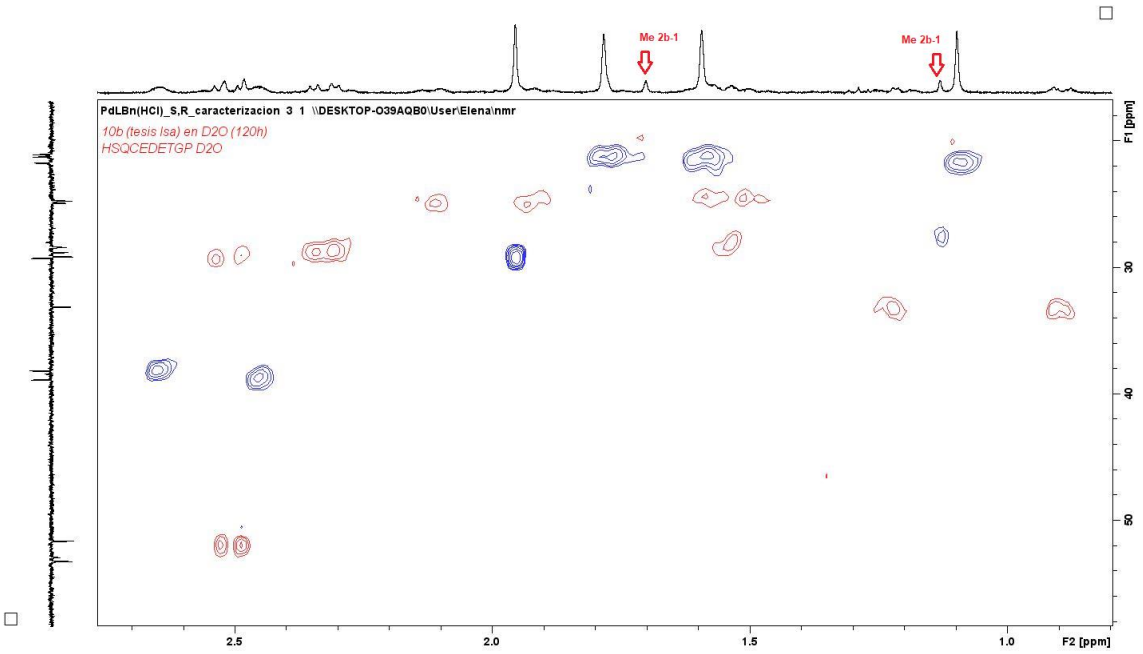

Figure S43. ^{15}N-^{1}H HMBC NMR spectrum of **2b-1** (*minor)* + **2b-2** (major) in water-d_2.

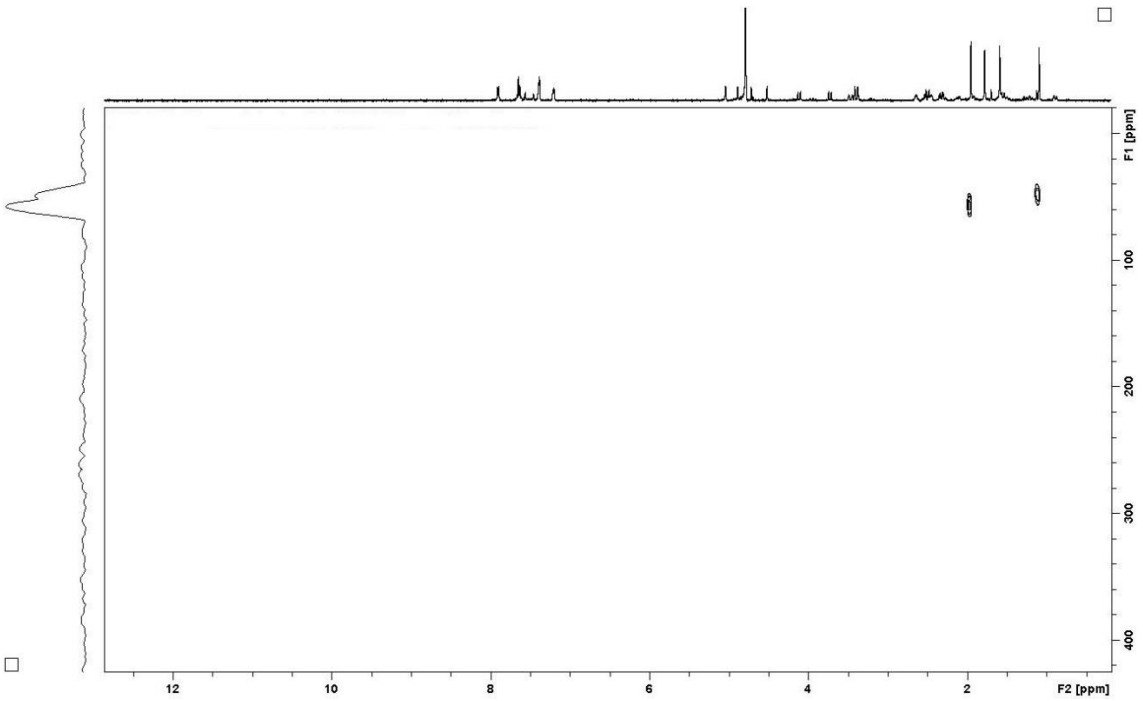

Figure S44. ^{13}C APT NMR spectrum of **2b-1** (minor) + **2b-2** (major) in methanol-d_4

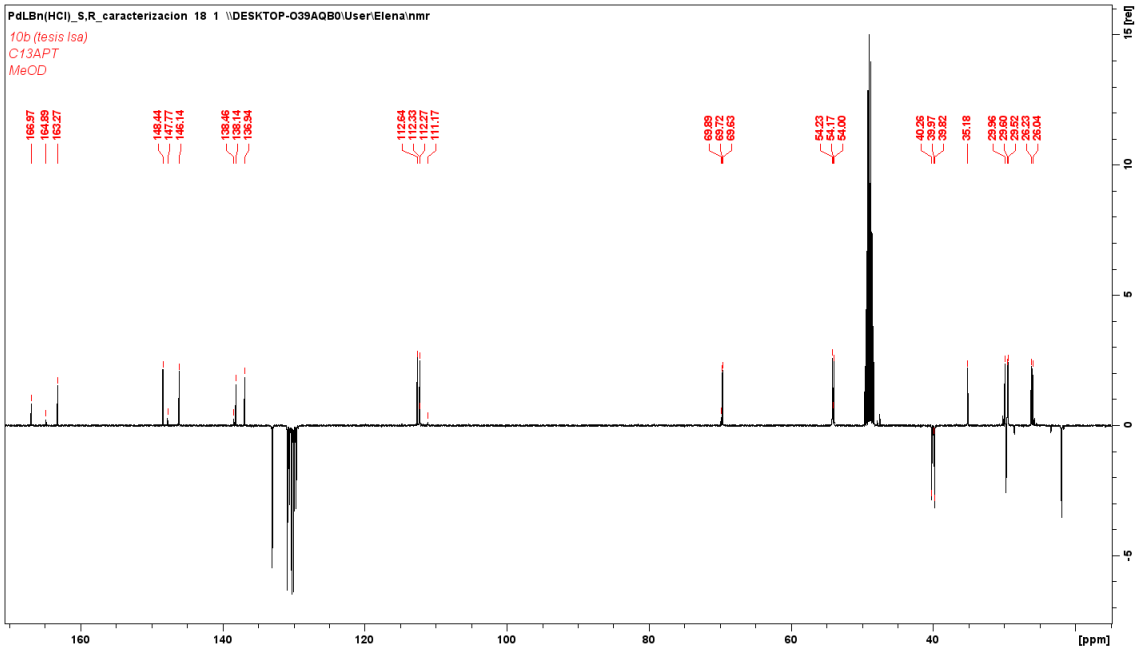

Figure S45. ^{1}H-^{13}C HSQC NMR spectrum of **2b-1** (minor) + **2b-2** (major) in methanol-d_4. Full and expanded

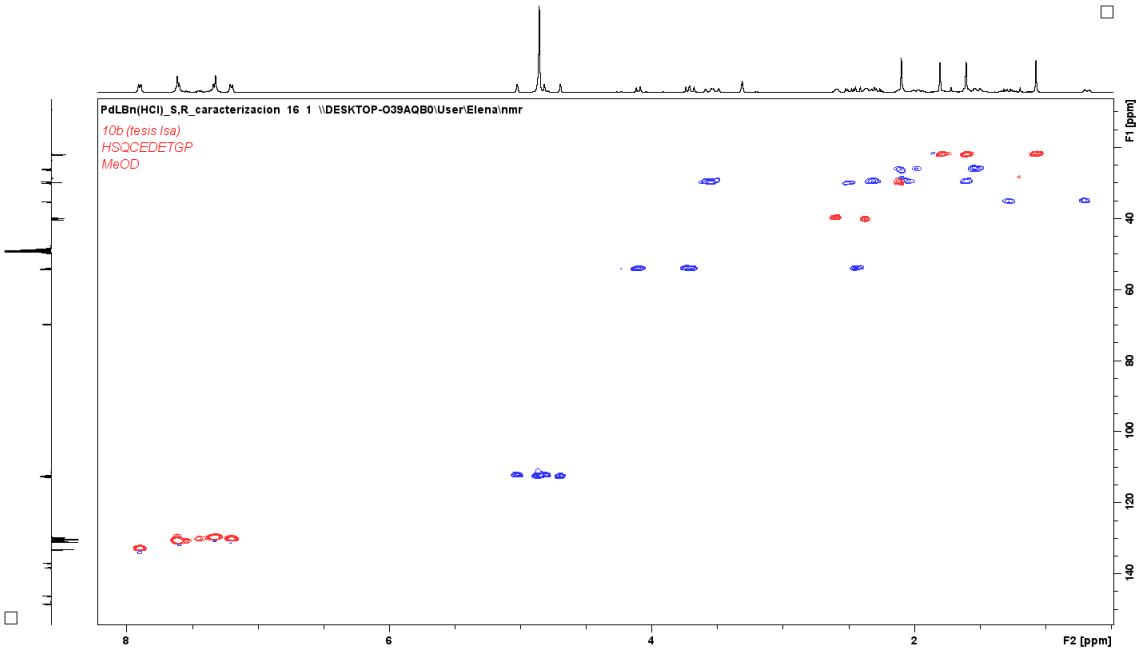

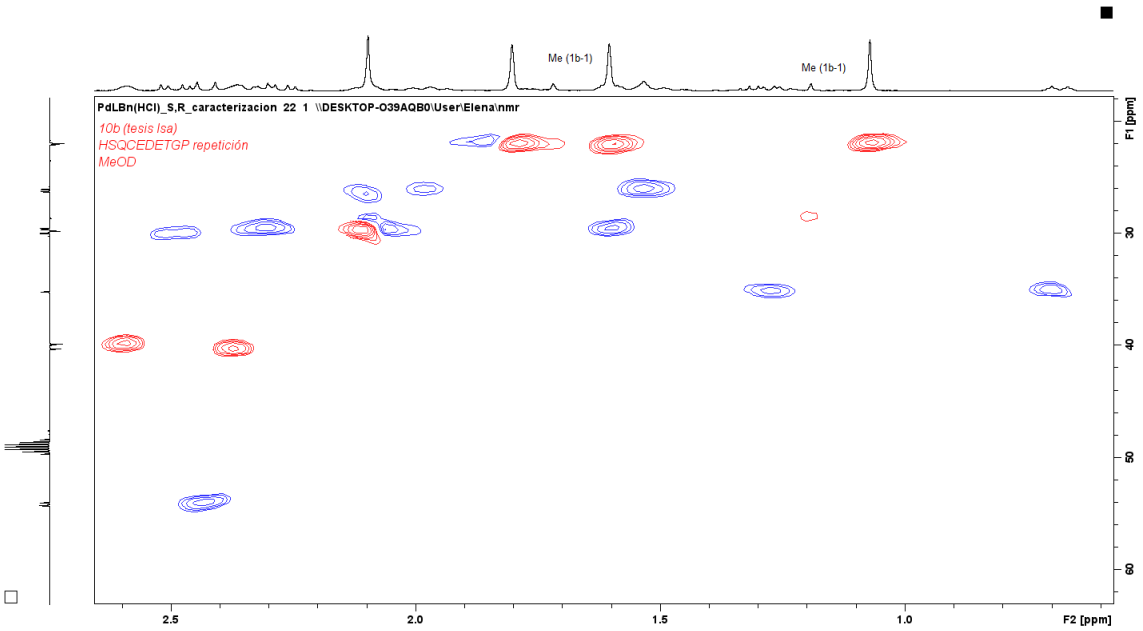

Figure S46. ^{1}H-^{15}N HMBC NMR spectrum of **2b-1** (minor) + **2b-2** (major) in methanol-d_4.

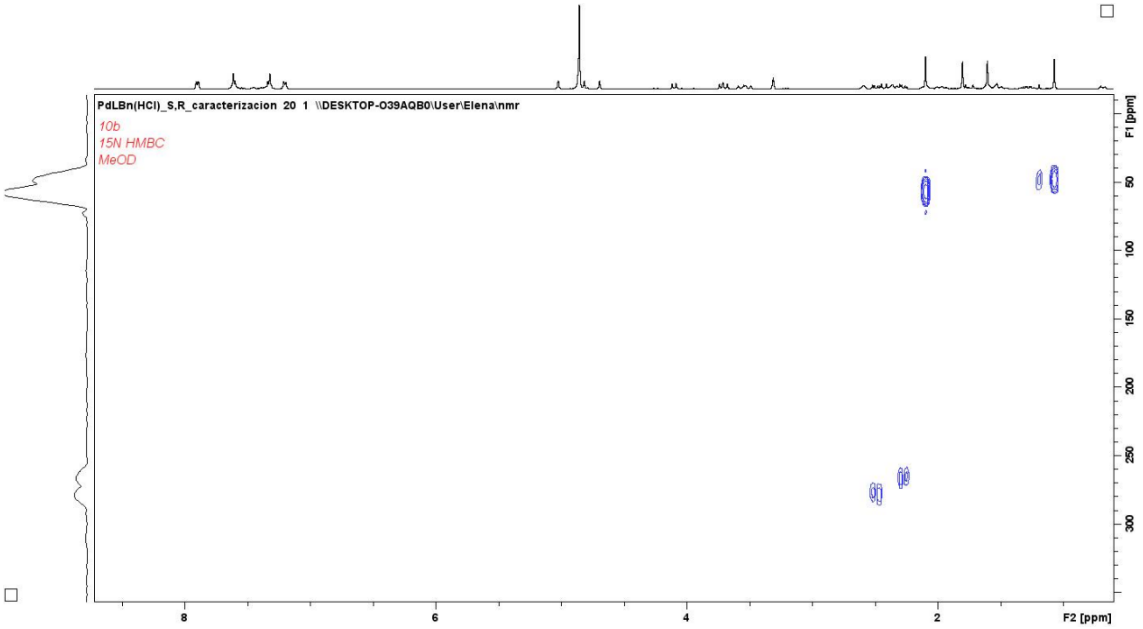

Figure S47. Time dependent UV-vis spectra in water of **1a** and comparison with UV-vis spectrum in water of **a·HCl.**

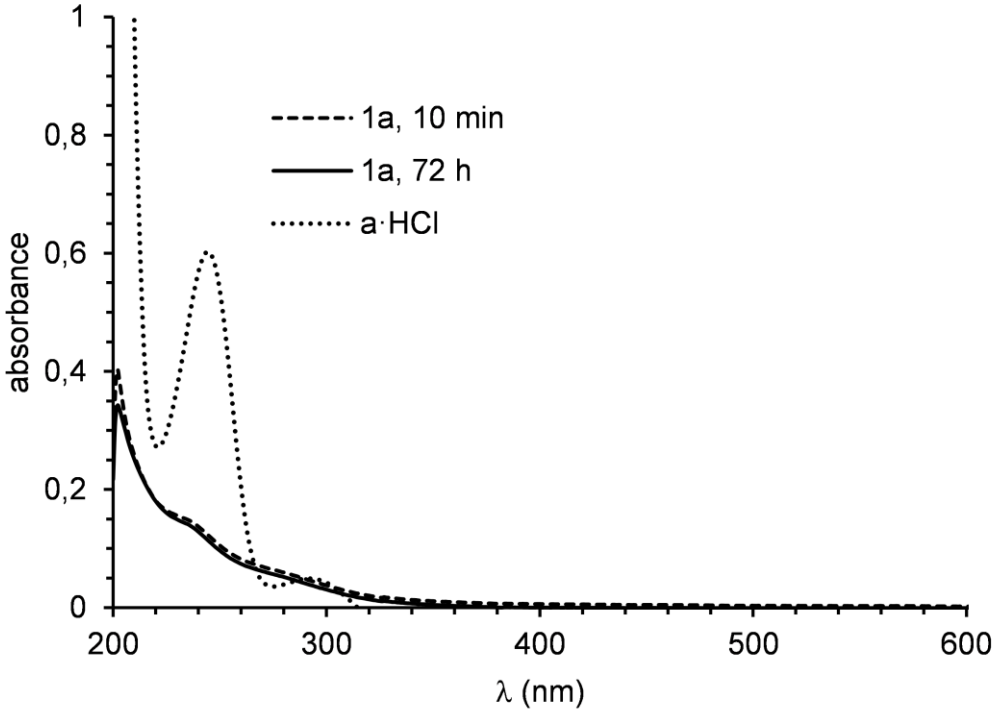

Figure S48. Time dependent UV-vis spectra in water of **1b** and comparison with UV-Vis spectrum in water of **b·HCl.**

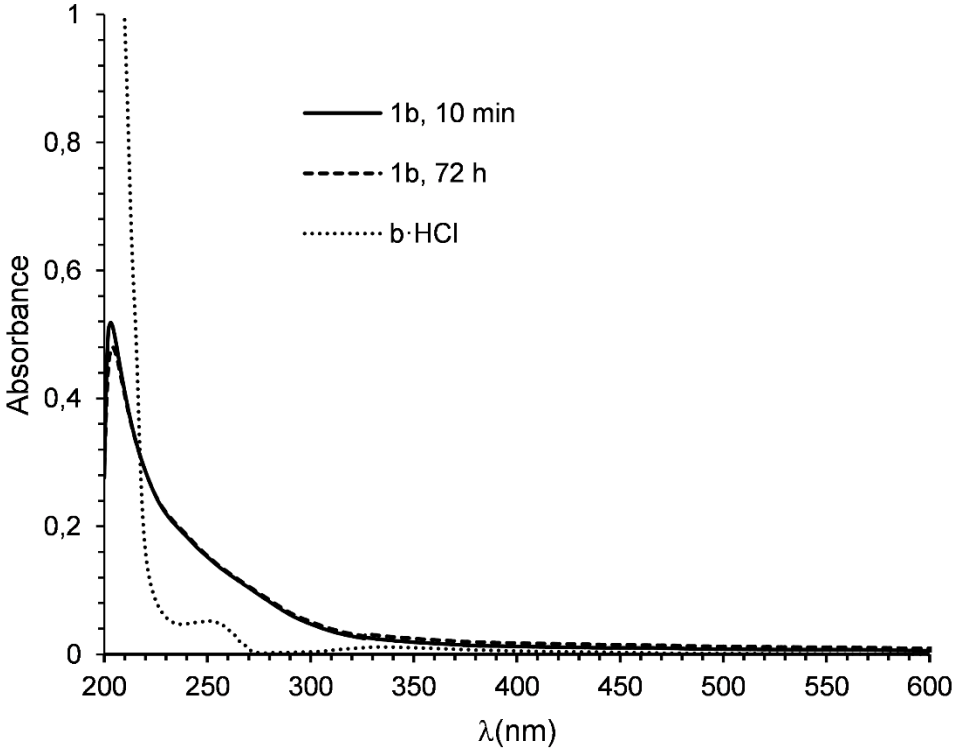

Figure S49. Time dependent UV-vis spectra in water of **2a**.

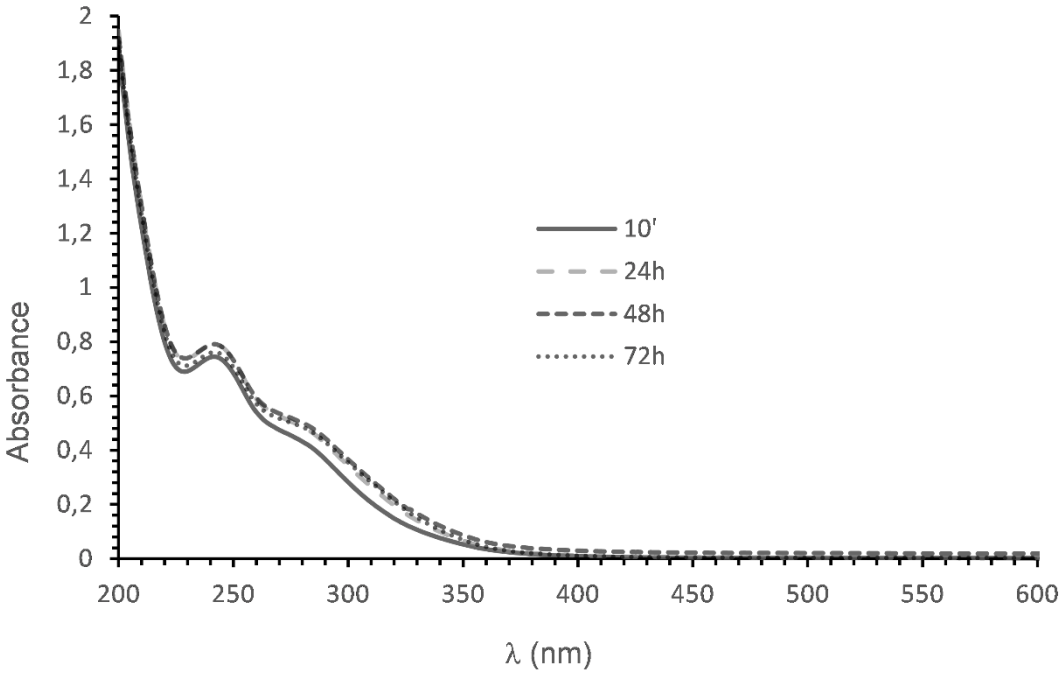

Figure S50. Time dependent UV-vis spectra in water of **2b**.

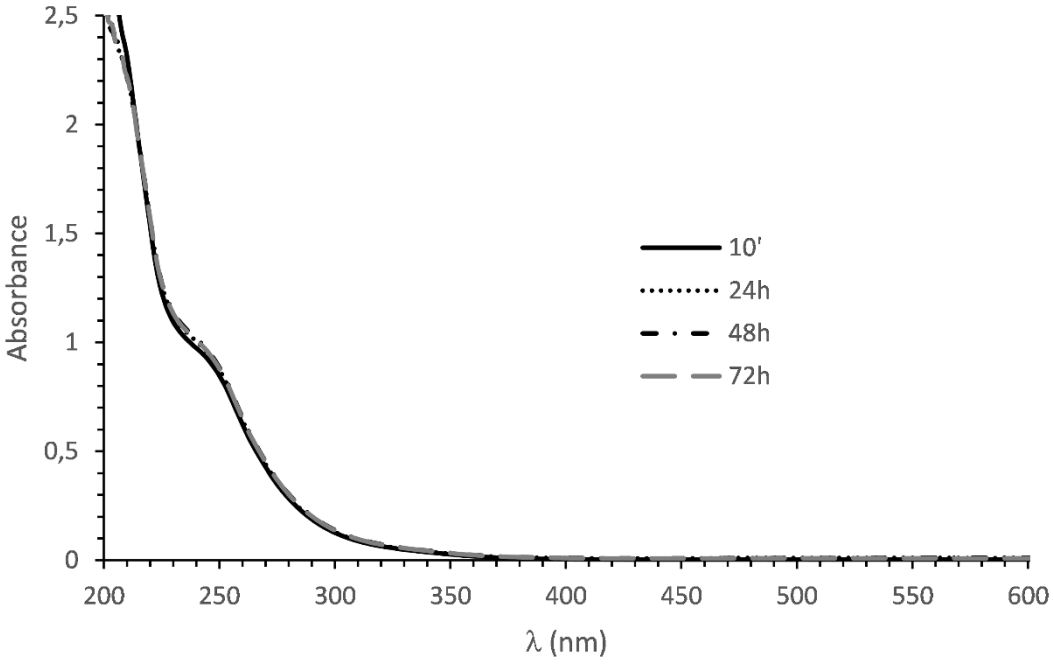

Figure S51. HR-ESI MS in water of **2a**, full spectra, expanded and simulated peak for ($C_{32}H_{43}N_4O_2Pd$), $[M\text{-}Cl]^+$.

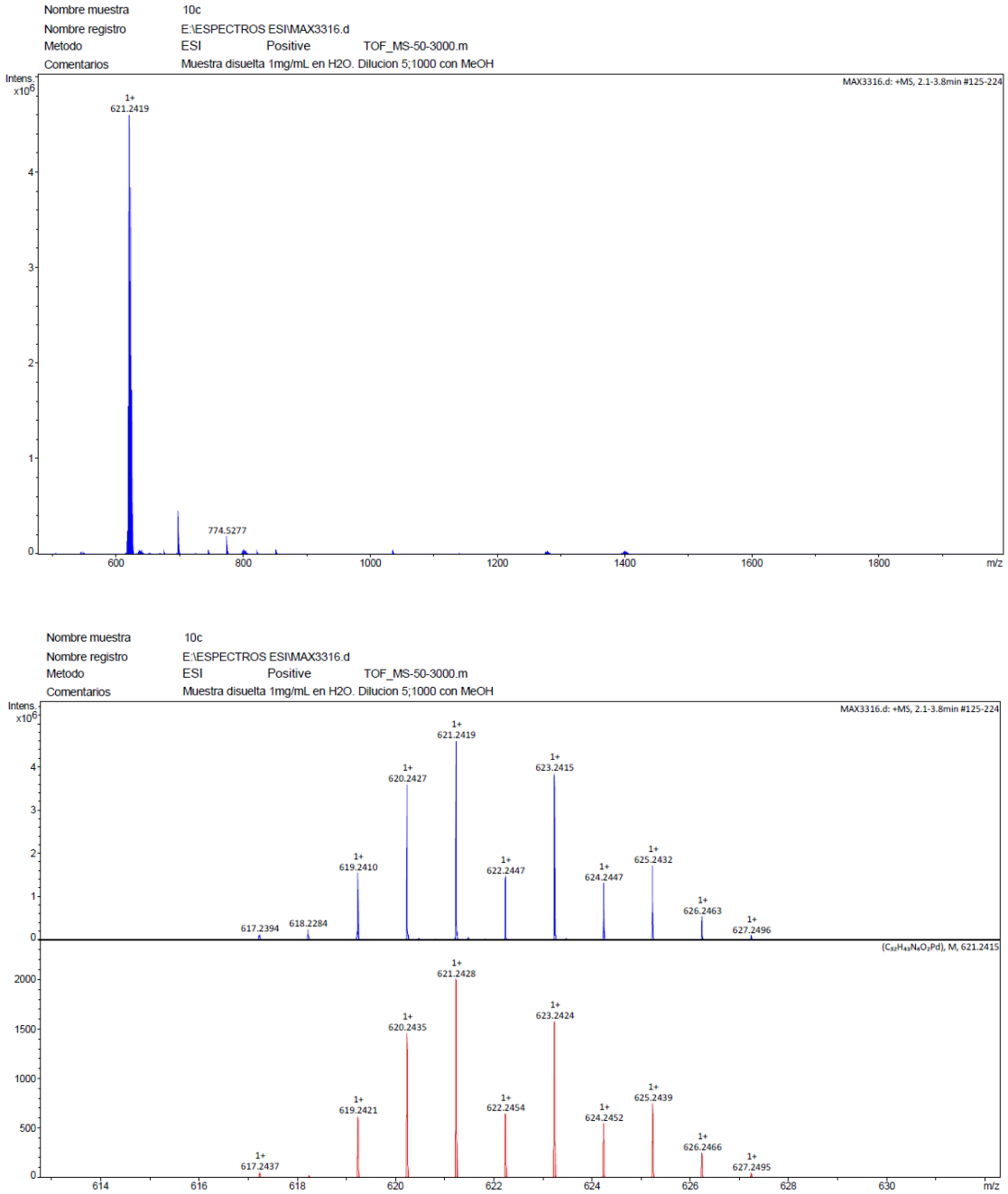

10c

MASA TEORICA	MASA EXPERIMENTAL	ERROR (ppm)	ERROR (amu)	
619.241	619.2421	-1.7764	0.0011	
620.2427	620.2435	-1.2898	0.0008	
621.2419	621.2428	-1.4487	0.0009	
622.2447	622.2454	-1.1250	0.0007	
623.2415	623.2424	-1.4441	0.0009	
624.2447	624.2452	-0.8010	0.0005	
625.2432	625.2439	-1.1196	0.0007	
626.2463	626.2466	-0.4790	0.0003	

Figure S52. HR-ESI MS in water of **2a'**, full spectra, expanded and simulated peak for ($C_{32}H_{43}N_4O_2Pd$), $[M\text{-}Cl]^+$.

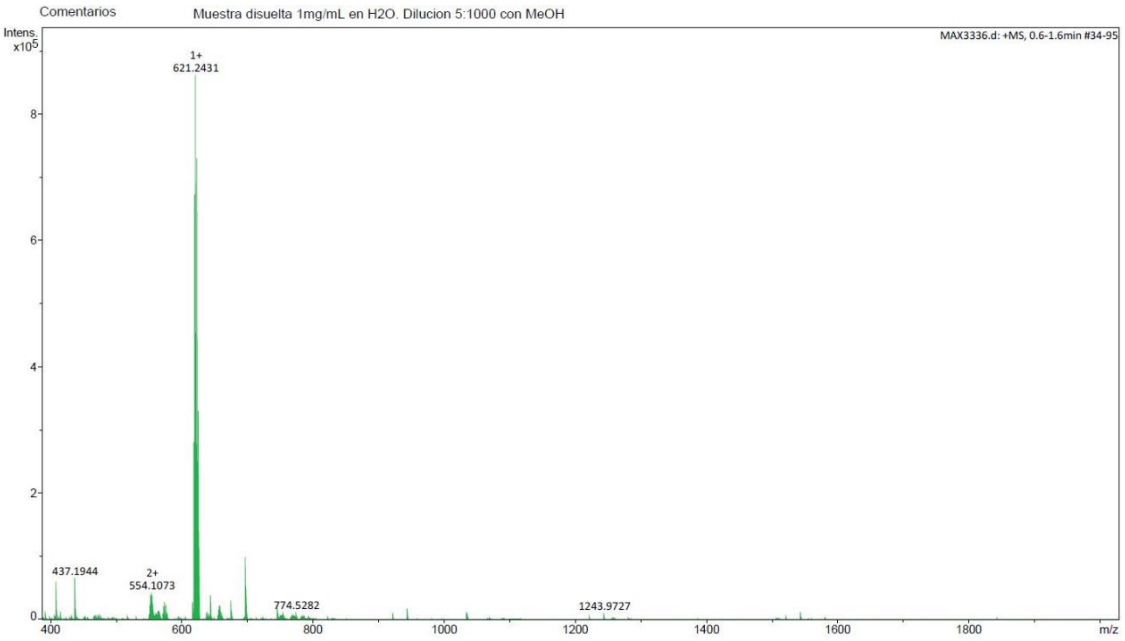

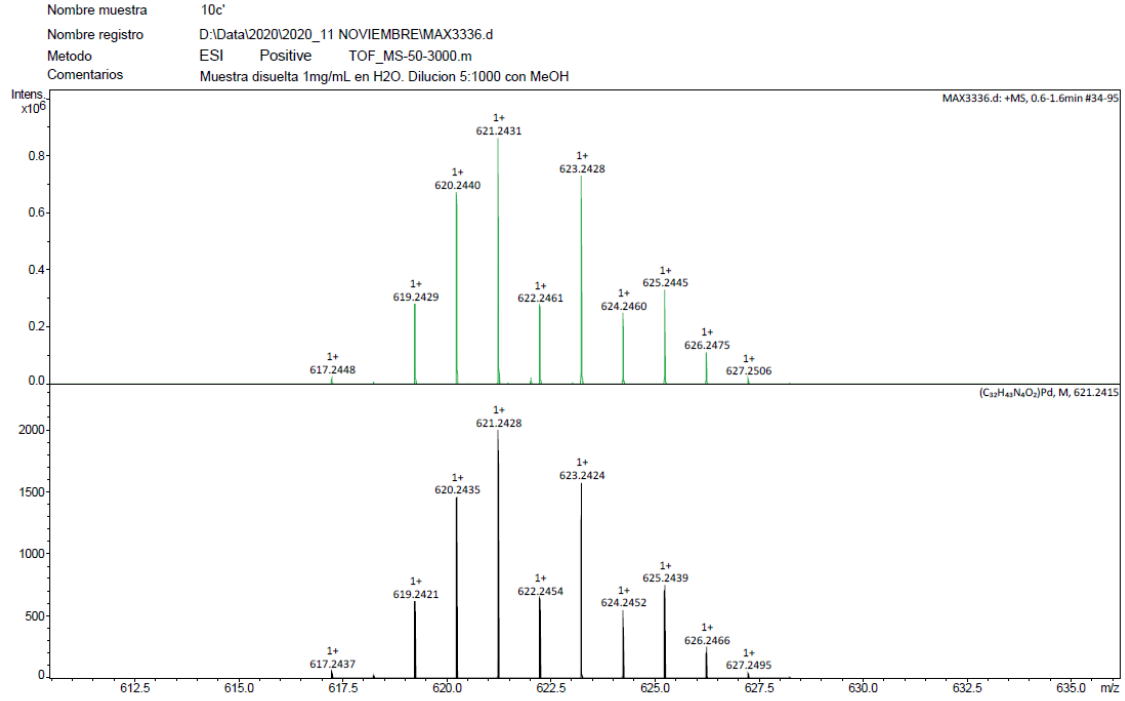

10c'

MASA TEORICA	MASA EXPERIMENTAL	ERROR (ppm)	ERROR (amu)	
617.2437	617.2448	-1.7821	0.0011	
618.2468	618.2478	-1.6175	0.001	
619.2421	619.2429	-1.2919	0.0008	
620.2435	620.244	-0.8061	0.0005	
621.2428	621.2431	-0.4829	0.0003	
622.2454	622.2461	-1.1250	0.0007	
623.2424	623.2428	-0.6418	0.0004	
624.2452	624.246	-1.2815	0.0008	
625.2439	625.2445	-0.9596	0.0006	
626.2466	626.2475	-1.4371	0.0009	

Figure S53. HR-ESI MS in water of **2b**, full spectra, theoretical and experimental mass for ($C_{34}H_{47}N_4O_2Pd$), $[M\text{-}Cl]^+$.

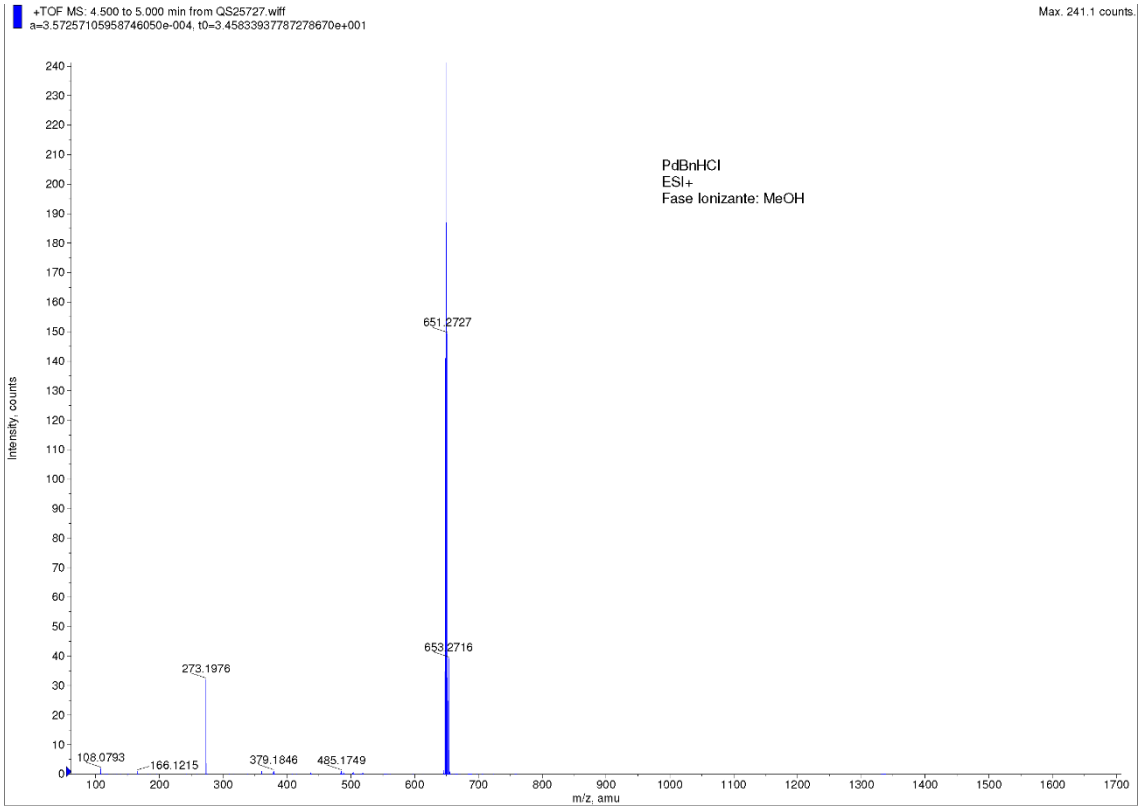

PdBnHCl

MASA TEORICA	MASA EXPERIMENTAL	ERROR (ppm)	ERROR (amu)	
647.2734	647.2733	0.1545	-0.0001	
648.2748	648.2756	-1.2340	0.0008	
649.2741	649.2749	-1.2321	0.0008	
650.2767	650.275	2.6143	-0.0017	
651.2738	651.2727	1.6890	-0.0011	
652.2766	652.272	7.0522	-0.0046	
653.2753	653.2716	5.6638	-0.0037	

Figure S54. FRET DNA melting curves of **2a**, **2a**', **2b** and **2b**'at 10 μM concentration with ds DNA (F10T, 0.2 μM).

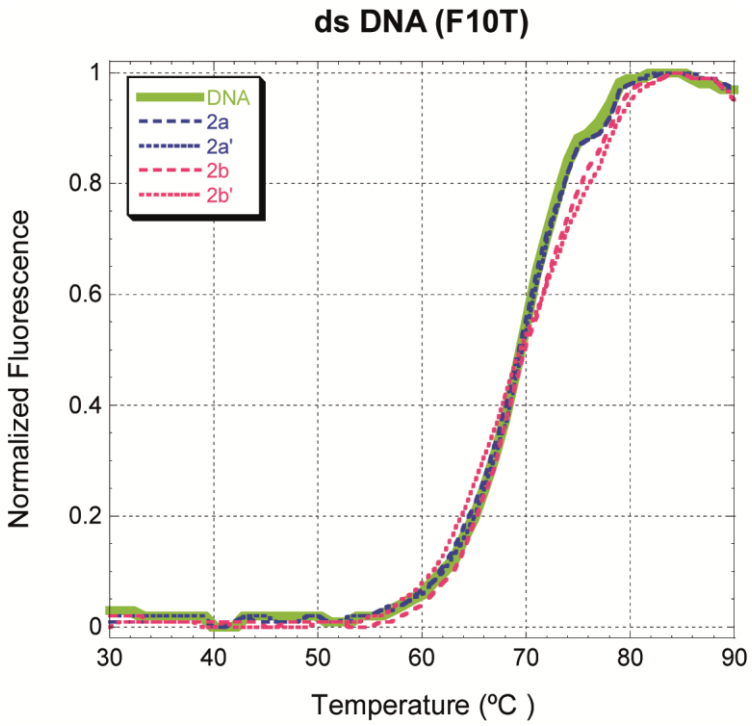

Figure S55: Analysis of cell cycle of PC-3 cells after treatment with cisplatin, **2a** and **2a'**. Cells were treated for 48 h with **2a** (0.79 µM) or **2a'** (0.17 µM). The results are shown as percentage of cells in each phase of the cycle as compared to untreated control cells. Data in the table are the means ± SEM of four independent experiments; *p < 0.05; ***p < 0.001 vs. control.

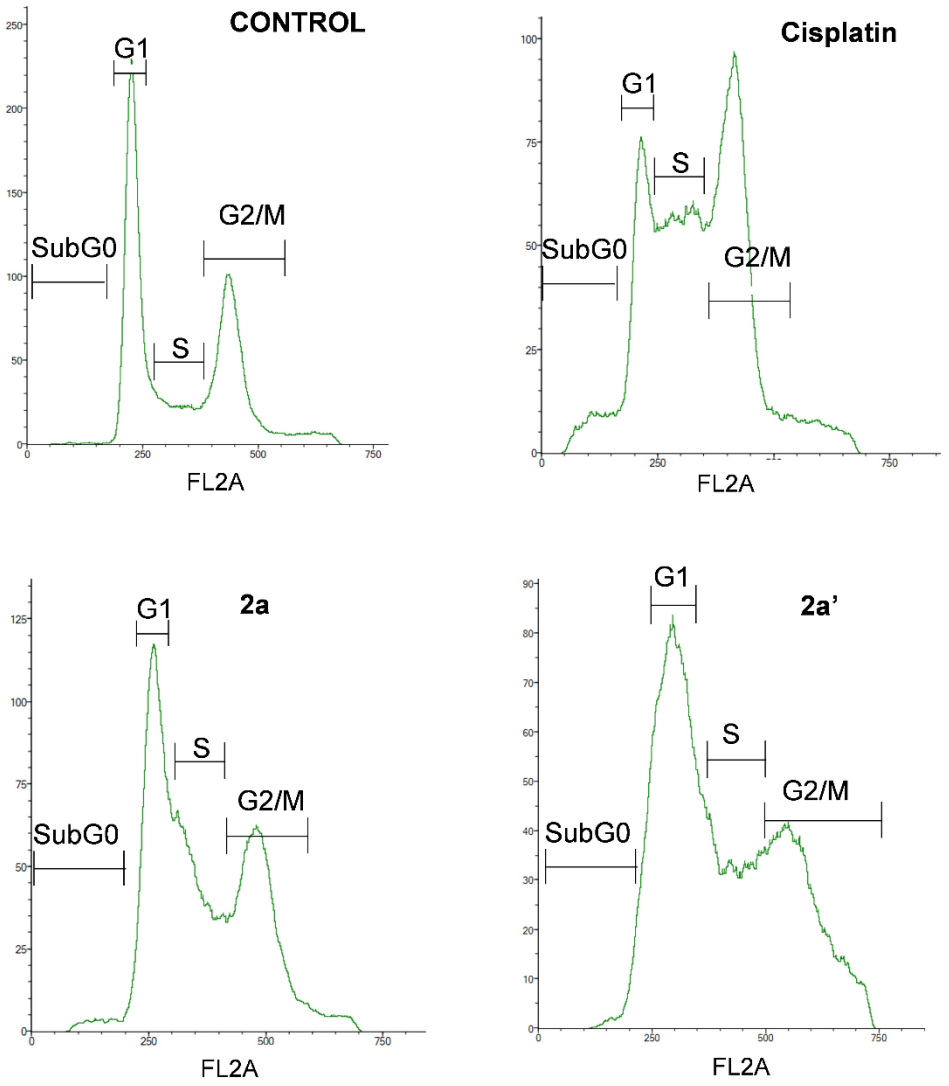

	SubG0	G1	S	G2/M
CONTROL	0.3 ± 0.01	63.64 ± 0.72	12.56 ± 0.33	23.87 ± 0.83
Cisplatin	4.5 ± 0.22***	22.88 ± 1.03***	37.02 ± 1.25***	38.34 ± 1.99***
2a	1.4 ± 0.78	48.59 ± 2.30***	18.82 ± 1.45***	32.58 ± 2.55***
2a'	2.4 ± 0.34*	37.99 ± 1.11***	21.13 ± 1.89***	40.64 ± 2.32***